CELLULAR IMMUNE RESPONSE AND GENE EXPRESSION PROFILING IN CROHN'S DISEASE PATIENTS ASSOCIATED WITH MYCOBACTERIUM AVIUM SUBSPECIES PARATUBERCULOSIS

by

CLAUDIA M. ROMERO
B.S. University of Los Andes, 1995
M.S. University of Central Florida, 2000

A dissertation submitted in partial fulfillment of the requirements
for the degree of Doctor of Philosophy
in the Burnett College of Biomedical Sciences
at the University of Central Florida
Orlando, Florida

Fall Term
2004

ABSTRACT

Despite the chronic debate in the etiology of Crohn's disease (CD), a debilitating inflammatory bowel disease (IBD) closely related to ulcerative colitis (UC), an emerging interest in a possible mycobacterial role has been marked. Granuloma and pathologic manifestations in CD resemble aspects found in tuberculosis, leprosy and paratuberculosis. The latter, a chronic enteritis in cattle, goat, sheep and primates, which is similar to human enteritis, also known as CD, is caused by a fastidious, slow growing *Mycobacterium avium* subspecies *paratuberculosis* (MAP). Due to the similarities between CD and paratuberculosis, a mycobacterial cause in CD has been proposed. Recent discovery of a possible association between NOD2/CARD15 mutations and risk of CD added support to microorganism-host interactions. In this study, a possible mycobacterial role in CD etiology has been evaluated by investigating the presence of MAP DNA, the state of the cellular immune response and microarray gene expression profiling in peripheral blood and surgical tissue from CD, UC and healthy control subjects. Nested PCR detected MAP DNA in tissue from 10/12(83%) CD patients compared to 1/6(17%) non-IBD subjects. Fluorescence *in situ* hybridization (FISH) with the aid of Confocal Scanning Laser Microscopy (CSLM) detected MAP DNA in 8/12(67%) CD subjects compared to 0/6(0%) in non-IBD subjects. The detection of MAP DNA by either technique in tissue from CD subjects is significant compared to non-IBD subjects ($P < 0.05$). MAP DNA was also detected in both inflamed and non-inflamed tissue from patients with CD suggesting MAP infiltration in human tissue. Correlation of possible MAP presence and the function of polymorphonuclear leukocytes (PMN) and peripheral blood mononuclear cells (PBMC) in 19 CD patients and 12 controls have

been evaluated. PMN phagocytosis of viable FITC-MAP was suppressed in 13/19(68%) CD patients compared to 0/12(0%) in healthy controls ($P<0.05$). PBMC phagocytosis of viable FITC-MAP was suppressed in 5/19(26%) of CD patients compared to 0/12(0%) of healthy controls ($P<0.05$). The proliferative response of PBMC with T-cell majority from CD and controls subjects was evaluated against PHA, *Candida albicans*, PWM and MAP PPD. Dysfunctional proliferative response against PHA was found in 8/19(42%) CD patients compared to 1/12(8.3%) in controls suggesting possible T-cell anergy. PBMC from 11 CD subjects reacted normally to PHA, 7/11(64%) reacted strongly to MAP PPD suggesting previous exposure to mycobacteria, and 3/11(27%) did not react with MAP PPD suggesting lack of pre-exposure to mycobacteria. From the seven mycobacterial pre-exposed samples, 6/7(86%) showed a normal ability to recall antigens by activated macrophages when exposed to *C. albicans*, and all 7 samples had a normal PWM response. Finally, microarray-chip technology was employed to identify the expression profile of genes that have a role in the immune response of CD patients. RNA was isolated from fresh buffy coats from 8 healthy controls, 2 CD, and 1 UC patients. Chips with an estimated of 30,000 human genes were hybridized to cDNA from these samples. We found that 17% of the total number of genes was differentially expressed. Over 200 genes were involved in the immune response, 7 genes where common to both forms of IBD (UC and CD), and 8 genes were found to be either downregulated in CD and upregulated in UC or viceversa. The IFNGR1 gene, which encodes the ligand-binding chain of the IFN-gamma receptor, was found to be downregulated in 2/2(100%) of CD patients, but not in UC patients. It is known that defects in IFNGR1 are a cause of atypical mycobacterial infection and bcg infection. Patients suffering from this deficiency have an immunologic defect predisposing them

to infection with mycobacteria. This correlates with the proposed theory as MAP being the causative agent of CD. Furthermore, the results indicate a host susceptibility requirement for the establishment of mycobacterial infection in CD patients. Further characterization of IFNGR1 using real-time PCR is underway. Collectively, detection of MAP DNA in the majority of CD tissue and the alteration in PMN and PBMC to respond efficiently to MAP may be related to the fact that mycobacterial pathogens infect phagocytic cells of susceptible hosts and consequently the immune response is dysregulated. Furthermore, the fact that a gene linked to mycobacterial susceptibility was found to be downregulated in CD patients only, strengthens the mycobacterial etiology of CD. In general, the data suggest a possible role for a bacterial pathogen in CD pathogenesis.

ACKNOWLEDGMENTS

Many thanks and appreciation to my advisor, Saleh A. Naser, who made all of this work possible. He persevered with me the whole time it took me to complete this research. To the members of my dissertation committee, Antonis Zervos, Henry Daniell, and Pappachan Kolattukudy, who have generously given their time and expertise to better my work. To UCF faculty for their knowledge and career training. To UCF staff, specially Sheryl Seaman and Rachel Franzetta, for providing guidance and advise to meet school requirements. To the members of my research laboratory for their constant support. To Ali Amirkhosravi and John Biggerstaff for their technical advise with the tissue work. To John Valentine and Ira Shafran for providing clinical samples. To William C. Nierman for his support and the microarray facilities. To Stanley H. Kim and Christine Shamblin for their technical advise with the microarray work. To the National Institutes of Health and the Wodzinski foundation for their financial funding. Finally, to my family and friends, specially my husband John Suarez, for his endless encouragement and patience.

TABLE OF CONTENTS

LIST OF FIGURES

LIST OF TABLES

LIST OF ACRONYMS

BrdU: Bromodeoxyuridine

CARD: Caspase-activation recruitment domain

CD: Crohn's disease

CMI: Cell-mediated immunity

CSLM: Confocal scanning laser microscopy

DC-SIGN: Dendritric cell-specific intracellular adhesion molecules

FISH: Fluorescence *in situ* hybridization

HSP: Heat shock proteins; NOD2

IBD: Inflammatory bowel disease

ICAM: Intracellular adhesion molecules

MAP: *Mycobacterium valium* subspecies *paratuberculosis*

NOD2: Nucleotide oligomerization binding domain 2

PBMN: Peripheral blood mononuclear cells

PCR: Polymerase chain reaction

PHA: Phytohemagglutinin

PMN: Polymorphonuclear leukocytes

PPD: Purified protein derivative

PWM: Pokeweed mitogen

TNF-alpha: Tumor necrosis factor alpha

UC: Ulcerative colitis

CHAPTER ONE: INTRODUCTION

Crohn's disease (CD) is a chronic inflammatory bowel disease (IBD) of controversial etiology with more than 500,000 people affected in the United States alone (27, 14). Although CD was initially described as a segmental disease of the small intestine, it has more recently been found to be associated with the mouth, larynx, esophagus, stomach, colon, skin, muscle, synovial tissue, and bone involvement (16, 17). The similarity in pathological manifestations and other aspects present in CD with those in animals diagnosed with paratuberculosis (also known as Johne's disease; JD) was first described by Dalziel (17) and later on by Chiodini (12). JD is a chronic inflammatory disease of ruminants caused by *Mycobacterium avium* subspecies *paratuberculosis* (MAP), a slow grower, fastidious and intracellular pathogen (74). Chiodini et al. isolated cell-wall deficient organisms, also known as spheroplast, from tissue of patients with CD following long term incubation culture (11). The spheroplast cultures then reverted to acid-fast mycobacterium-like organism after a single *in vitro* passage (10, 11). They were confirmed as MAP culture using IS900 probe (55). This was followed by several studies, which resulted in mixed results (18, 33, 52, 57, 59, 71, 76, 82, 86). Although, the culture methodology remains the most sensitive and convincing approach for confirming or excluding a mycobacterial role in CD etiology, this approach faces many obstacles related to the fastidious characteristics and lack of cell wall of the MAP bacterium in human CD tissue. There is a need for additional methodologies where MAP may be identified directly in tissue specimens. As reported in the literature, regions in the 1.451 kb IS900 sequence remain to be unique to MAP (33). Ultimately,

these IS900-derived nucleotide sequences may be used as markers for verification of MAP involvement in tissue (7, 40), and in milk from patients with CD (62).

Patients with CD tend to have abnormalities in the immune system, but it is not clear whether these abnormalities are cause or result of the disease. There are a variety of cellular processes and pro-inflammatory mediators that influence the pathogenesis of the disease. It is believed that there is a continuous immune response in the gut in response to an environmental stimuli.. CD has been classified into two distinct disease subtypes: a perforating form and a non-perforating form (34, 40, 57). This dual clinical presentation also renders CD analogous to two other mycobacterial diseases, leprosy and tuberculosis, which both manifest in two distinct clinical forms: a contained form and an aggressive form. (35, 80, 85). As with tuberculosis and leprosy, the various manifestations of the infections are attributable to the interactions with, and the plasticity of, the immune response (80). Many of the systemic findings are attributable to the pro-inflammatory cytokines that are released (IL-1, TNF-alpha, etc). MAP may be resistant to killing by macrophages and/or PMN, and *M. avium* has been shown to be resistant to killing by dendritic macrophages (58). Given the similarities between tuberculosis and CD, T-cell anergy as a result of persistent antigen stimulation may be relevant to granuloma formation and inflammation in CD disease. Further evidence that supported the role of MAP in CD etiology was reported including the detection of anti-MAP IgG antibodies in sera from significant CD patients compared to controls (23, 61, 77).

In 2001, the first susceptibility gene for CD, NOD2 (nucleotide-binding oligomerization domain), was identified (43, 68). NOD2 is expressed in the cytoplasm of monocytes, and it is comprised of N-terminus caspase-activation recruitment domains (CARD), a central nucleotide-

binding domain, and a C-terminus leucine-rich repeat (LRR) domain. The LRR domain is required for NOD2 signaling in response to muramyl dipeptide (MDP), the minimally active component of bacterial cell wall peptidoglycan. Mutations in NOD2 gene have been shown to be associated with CD, suggesting a role for intracellular pathogen-host interactions in the etiology of CD. Genetic defects, which result in modification or inactive cytokines or signaling molecules, may also disrupt immune function (20, 67). A point mutation in the coding region of the gene for interferon-gamma receptor 1 results in a new stop codon and in the production of a truncated protein that results in failure of interferon-gamma to stimulate proper antigen processing and presentation and increased susceptibility to mycobacterial infection (46).

Rationale for the study

The mystery of IBD with regard to etiology and pathogenesis led to controversial approaches in diagnosis and treatment of these diseases. Ultimately, IBD sufferers are subjective to the knowledge and expertise of their attending physicians. Consequently, the treatment of patients with IBD may vary from one clinic to another and from geographic region to the next. There is an immediate need for focused research that may unravel the mystery of IBD, especially CD. Unraveling the etiology of CD will go a long way toward targeted treatment and ultimately curing the disease rather than containing it. The purpose of this work is to comprehensively study the mycobacterial etiology, as has been proposed in the literature, of CD by investigating possible resemblance in immunological events that occur in tuberculosis and CD patients. Subjects enrolled in this study were approved by IRB (institutional review board) regulation at the University of Central Florida and University of Florida. Accordingly, coded peripheral blood

and tissue samples were collected, processed and analyzed. Specifically, clinical samples from patients with CD, UC, non-IBD and healthy controls were used to investigate the presence of MAP DNA, immunogenicity of immune cells and to study gene expression profiling. Ultimately, better understanding of mycobacterial association with CD may be determined. The impact of this research will be tremendous on millions of IBD sufferers in terms of diagnosis and treatment.

CHAPTER TWO: EVALUATION OF SURGICAL TISSUE FROM PATIENTS WITH CROHN'S DISEASE FOR THE PRESENCE OF MYCOBACTERIUM AVIUM SUBSPECIES PARATUBERCULOSIS DNA BY IN-SITU HYBRIDIZATION AND NESTED PCR

Introduction

In situ detection of nucleic acid sequences provides a direct visualization of the spatial location of specific sequences that is important for diagnosis of bacterial and viral infections (63). Confocal scanning laser microscopy (CSLM) is a technique where the specimen is illuminated by a focused beam of light. An image is recorded by scanning the beam of light over the specimen, and the reflected or fluorescent light from the specimen is focused onto a small detector aperture. This combination of point illumination and point detection results in a unique "optical sectioning" capability. This optical sectioning makes it possible to record images of thin layers within the specimen without cutting it into slices. By collecting a "stack" of such images from different depths, it is possible to display and quantify the three-dimensional structure of a specimen (3). In this chapter, we have employed both fluorescence *in situ* hybridization using a specific MAP DNA probe and CLSM and two rounds of nested PCR in an attempt to investigate the presence or absence of MAP DNA in surgical tissue specimens from patients with CD, ulcerative colitis (UC) or non-IBD.

Methods and Materials

Tissue Collection

A total of 31 surgical resectioned full-thickness tissue specimens including 23 tissues from 12 CD subjects (consisting of 12 inflamed and 11 non-inflamed tissue), 2 inflamed tissue from 2 patients with UC and 6 cancerous tissue samples from 6 patients with colon cancer, were included in this study. Coded tissue specimens were obtained at the time of surgery from consented participating subjects following Institutional Review Board (IRB) Regulation. The diagnosis CD or UC was established following standard clinical, endoscopic, histologic, and radiographic criteria (72). Disease activity was determined by use of the Harvey-Bradshaw index (37) and/or the clinical impression of the treating physician. The tissue specimens were kindly provided either by Dr. I. Shafran (Florida Hospital. Orlando, Florida) or by Dr. J. Valentine (University of Florida and Gainesville VAMC, Gainesville, FL). Samples representing inflamed and non-inflamed areas of the bowel from CD patients were sought. Colonic specimens from UC and other non-IBD patients that are undergoing colectomy or partial colectomy were also sought and used as controls. The tissue samples were examined macroscopically upon arrival, removed from the transport tube, flash frozen and stored in liquid nitrogen. Table 1 summarizes the demographic data related to subjects including disease history, use of immunosuppressive and the type of tissue samples used in the study.

Tissue Sectioning and Processing

Tissue specimens were removed from liquid nitrogen, placed in the cryostat, left for 30 min to equilibrate at –20 ^{0}C, placed onto cryostat tissue holders and embedded in mounting medium (OCT embedding medium, RA LAMB, NC). A total of 20 serial 20 um sections from each tissue specimen were cut, placed on 20 microscope slides, and allowed to air dry. All slides containing tissue sections were fixed in 4% PFA (Sigma, MO) for 30 minutes at room temperature. Under the same conditions, slides were then washed 3 times in PBS (pH 6.8). Tissue sections were permeabilized with 100uL (20ug/mL) of Proteinase K (Sigma, MO) and 1% of SDS for 30 min at 55^{o}C. Proteinase K was then inactivated with 200 uL of 0.2% glycine (Fisher Scientific, CA) for 3 min, and slides were then washed 3 times in PBS (pH 6.8). Tissue sections were dehydrated in 1 minute washes of 70%, 90%, and 100% ethanol. Sections were then washed for 1min with 100% xylene (Fisher Scientific, CA) to remove excess lipids. Tissue sections were re-hydrated with 1 m washes of 100%, 90%, and 70% ethanol and incubated in PBS (pH 6.8) at room temperature for 1 hour. Finally, sections were incubated in 25 mL of pre-hybridization solution (2X SSC, 20% dextran sulfate, and 50% formamide) for 5 min at 50^{o}C immediately before hybridization. MAP cultured in our laboratory from CD tissue was used as a positive control to optimize the protocol conditions. MAP was grown in MGIT media as described previously (76). Growth was observed as non-homogenous turbidity in approximately 8 weeks. A volume of 0.05 mL was aseptically removed from the culture to a sterile 1.5 mL microcentrifuge tube and centrifuged at 10,000 rpm for 10 minutes at 4 ^{o}C. The cell pellet was washed 3 times in PBS (pH 6.8) and then resuspended in 0.10 mL PBS, with 20 uL aliquoted to

each slide. Several slides containing thin smear were prepared and then allowed to air dry in a Biosafety class II cabinet for 1 hour. Slides were then heat fixed at 70 ^{o}C for 1 hour.

Quality controls

The FISH protocol was optimized earlier in the study by testing sections from normal tissue of colon cancer patients that were spiked with MAP ATCC strain 43015 and tissue sections without the spiking with MAP. The specificity of the IS900-labeled probe was tested using slides containing no bacterial smear, *Escherichia coli*, *Mycobacterium smegmatis*, *Mycobacterium avium subspecies avium*, *Staphylococcus aureus* and MAP.

Probe Preparation and hybridization

A 20-mer MAP specific oligonucleotide probe (5'-CTTCGGGGCCGTCGCTTAGG-3') derived from the IS900 sequence was labeled at the 5'-end with fluorescein (Invitrogen, CA). Aliquots of 1ug/uL were stored at –20^{o}C. One hundred nanograms of fresh probe were mixed with 20 uL of hybridization solution (1% Triton X-100, 2X SSC, denatured sperm DNA (500 ug/mL), 10% dextran sulfate, and 50% deionized formamide), boiled for 10 min and placed on ice for 10 more minutes. The hybridization mixture was added to the tissue sections and placed inside a hybridization chamber (Corning inc., MA) overnight at 37^{o}C. After 24 h, tissue samples were removed from the chamber and extensively washed. The first wash was with 2X SSC for 15 min at room temperature, followed with another wash with 1X SSC under the same conditions. The last 2 washes were done with 0.3X SSC, one for 15 min at 40 ^{o}C, and the other one for 15 min at room temperature. Slides were then incubated in 40 mL of counterstain

solution containing 40 ng of propidium iodide (Sigma, MO) for 15 min at room temperature in the dark. Slides were then washed three times with sterile water each time for 5 min at room temperature, and air-dried in the dark. Slides were then mounted with anti-fade solution (Molecular Probes, OR) before storage to preserve the fluorescence.

Confocal Scanning Laser Microscopy Analysis

A Carl Zeiss LSM 510 system was used in this study (Carl Zeiss Inc., NY). Slides were examined to localize the targets on the slide by using transmitted-light. Once the target was found, two simultaneous confocal channels were used for reflection and fluorescence. The detector on the microscope was set to include light from the negative control, and was kept constant for all test samples. All variables, such as photometric gain, photomultipler setting, pixel size, objective size, and number of scans were recorded for each scan and were used comparatively for sample slides. Using the Zeiss image analysis software, a treshold was applied to eliminate pixels with no fluorescence (black) and residual noise from the detector. Images with relevant data were saved for documentation.

Statistical analysis

Groups were compared in using 2x2 contingency tables and Fishers Exact test. Significant data had a P value < 0.05.

Genomic DNA Extraction and Nested PCR Analysis

Approximately five hundred mg of fresh tissue was diced into fine pieces using sterile disposable scalpels. The tissue sample was re-suspended in 4.0 ml of lysis buffer (2mM EDTA, 400 mM NaCl, 10 mM TrisHCl pH8, 100 ug/ml Proteinase K, and 0.6% SDS) and homogenized by an Omni Tip disposable generator probe (Fisher Scientific Pittsburgh, PA) for 1 min at 30,000 rpm. The tissue was then incubated with shaking (200rpm) at 37°C for 3 hrs, transferred to disposable FastPrep® lysing matrix B blue cap tube (Qbiogene, Carlsbad, CA), and ribolysed at $6.5m/s^{-2}$ for 45secs by using a FastPrep® ribolyser (Qbiogene, Carlsbad, CA). The lysates were placed on ice immediately for 15min. The DNA was then isolated by phenol/chloroform/isoamyl alcohol and ethanol precipitation. DNA pellet was dissolved in 250 µl TE buffer. The MAP specific IS900 DNA element was evaluated in triplicate using a nested primer PCR technique. Briefly, oligonucleotide primers P90 (5'-GTT-CGG-GGC-CGT-CGC-TTA-GG-3') and P91 (5'-GAG-GTC-GAT-CGC-CCA-CGT-GA-3') were selected to amplify a unique 398 bp fragment of 5' region of IS900. To reliably detect MAP, AV1(5'-ATG-TGG-TTG-CTG TGT-TGG-ATG-G-3') and AV2(5'-CCG-CCG-CAA-TCA-ACT-CCA-G-3') were used for the nested PCR in the second round using the amplified fragment as a template to amplify a 298 bp internal sequence. The PCR reaction mixture of 50 µL consisted of 1×PCR buffer, 5mM $MgCl_2$, 0.2mM dNTP, 6% DMSO or 0.5M Betaine, 2µM primers, and 2.5u Platinum Taq polymerase (Invitrogen Carlsbad CA) and 10µl of DNA template. Five µl of DNA template was used in first around PCR reaction in 50µl. 1µl of PCR product from first round was used in second round PCR in 50µl. The PCR cycling conditions were as follows: 95°C for 5 min,

40cycles of 95°C for 1min, 58°C for 1min, 72°C for 3 min; and a final extension of 5 min at 72°C. The amplification product size was determined on an agarose gel. Some of the nested PCR products were gel purified and sequenced by the University of Florida DNA Sequencing Core facility confirming that the product was identical to the MAP IS900 sequence.

Results

A total of 20 patients who underwent for surgery for resection of bowel tissue were enrolled for this study between July 2002 and January 2004. Twelve patients were diagnosed with CD, 2 with UC and 6 with colon cancer (non-IBD). The median age was 41 yr for CD patients and 52 yr for non-CD patients equally distributed as males and females. The data in Table 1 shows that 11 out of 12 (92%) CD patients were on immunosuppressive medications, Neither of the 2 patients with UC nor the 6 non-IBD controls were on immunosuppressive medications.

Specificity of the IS900-Based FISH

Using slides containing cultures representing MAP, *M. smegmatis*, *M. avium* subspecies *avium, Staphylococcus aureus* and *E. coli* were used to test the specificity of the FITC-labeled IS900-derived DNA probe. As shown in Fig. 1, the presence of MAP was detected as a yellow color indicating the colocalization of the FITC-green fluorescence labeled-IS900 probe hybridized with corresponding MAP DNA present in the bacterial samples (E). Slides containing *E. coli* (A), *Staphylococcus aureus* (B) and *M. smegmatis* (C) and *M. avium* subspecies *avium* (D) cultures were negative against the FITC-labeled IS900 probe. Hybridization signals with

MAP DNA were detected mostly in clumps distribution, a typical characteristic of mycobacterial morphology following microscopic staining. Slides without any bacterial smear were blank (data not shown). All the variables mentioned above including various dilutions of bacterial cells and probes were repeated several times with duplicate slides in every attempt. The results remained consistent at all times. After several attempts for adjustment of variables, parameters were identified and then employed during this study. MAP was absent in slides containing sections from normal tissue of a colon cancer patient when analyzed using the optimized protocol described earlier (Fig. 2A). However, MAP in clumps was clearly visualized in slides with tissue sections spiked with MAP culture (Fig. 2B).

Detection of MAP DNA in Tissue by FISH and CSLM

Slides containing CD and non-CD tissue sections were used, and the presence of MAP was detected as a yellow color indicating the specific hybridization of the green fluorescent MAP probe with the MAP DNA present in the red stained human tissue samples. For the isotypic control slides, PBS was used instead of MAP probe to establish the threshold to eliminate residual noise during image analysis. In 12 CD patients tissue, MAP DNA was detected in 7/12 (58%) of inflamed, 4/11 (36%) of non-inflamed and in 8/12 (67%) of either tissue type (Table 2). Fig. 3 illustrates representative CLSM images of tissue sections from CD patients following hybridization with the IS900 probe; MAP DNA was detected only in inflamed tissue (A:I), only in non-inflamed tissue (B:N) and in both inflamed and non-inflamed tissue (C:I and C:N). MAP infiltration was observed in three CD patients since both tissue types contained MAP DNA. On the contrary, MAP DNA was absent in both Tissue types in two CD patients. As shown in Fig.

4, MAP DNA was not detected in tissue sections from all six non-IBD patients (A to F). Detection of MAP DNA by FISH in 67% of CD tissue compared to zero in non-CD tissue is significant ($P < 0.005$).

Detection of MAP DNA in Tissue by Nested PCR

In order for low level of MAP DNA to be specifically detected, the second round of the nested PCR technology was employed in this study which amplifies an internal 298 bp fragment from a template of 398 bp fragment amplified in the first round of the PCR. An intense bright band has been observed in all positive results. The amplified fragment was confirmed to be IS900 by nucleotide sequencing. . In this study, a total of 31 DNA extracts isolated directly from homogenized 31 tissue samples were analyzed. As shown in Table 2, MAP DNA was detected in tissue from 10/12 (83%) of CD subjects, 2/2 (100%) inflamed tissue from 2 UC patients compared to 1/6 (17%) of non-IBD subjects ($P<0.005$). Interestingly, MAP DNA in CD tissue was detected in 7 inflamed samples (Fig. 5A, lanes 4, 8,10, 14 and Fig 5B, lanes 4, 6, 8) and in 6 of non-inflamed samples (Fig. 5A, lanes 3, 5, 11, 13, 15, and Fig. 5B, lane 3). MAP DNA in non-IBD tissue was detected in two tissue samples (Fig. 5B lanes 9 and 10).

Discussion

We used a direct analysis in this study, which investigates the presence or absence of MAP DNA in tissue. We used two sequential rounds of nested PCR, on DNA preparations extracted directly from tissue samples, in order to substitute for Southern hybridization. The use of FISH with the aid of CSLM may provide physical evidence of the MAP bacterium in human

tissue and thus become essential in investigating any link between MAP and CD. The FISH methodology employed in this study has been carefully optimized to provide significant sensitivity and specificity to the MAP bacterium. As shown in this study, spiking of normal tissue with MAP culture was clearly evident in the slides following our protocol (Fig. 2B). When coded tissue sections were investigated by FISH, MAP presence was easily reported. The data shown in Fig. 3 illustrates that MAP may be present in inflamed tissue, neighboring non-inflamed tissue or in both. While accepting a possible sampling error during tissue collection and coding, MAP presence in inflamed tissue only in CD patients goes well with the general wisdom. Detection of MAP DNA in non-inflamed and not in the inflamed tissue samples may be explained by several scenarios including sampling error, poor inflamed tissue quality or low number and diversity in the distribution of MAP in the inflamed tissue. Detection of MAP in both the inflamed and non-inflamed tissue samples suggests that MAP infiltrates host tissue as reported in animals with JD (36). Ultimately this confirms that MAP infection in human is systemic as we reported earlier when MAP was cultured in milk from CD patients (62). This was also confirmed most recently in a new report where viable MAP was cultured from peripheral blood of 50% CD patients (64). On the contrary, MAP may be absent in some CD patients as we reported in this study where MAP DNA was not detected in tissue by either technique. It is also of significant importance to report that MAP may be present in some patients with UC. A study reported isolation of pleomorphic variable acid-fast organisms in over 50% of UC patients (60). Furthermore, Mishina et al reported that 2/4 UC tissue where MAP positive by RT-PCR (57). In this study, two inflamed UC tissue had MAP DNA by nested PCR. We regret that FISH was not performed on the UC tissues samples due to the small size of tissue

samples. MAP in tissue from UC patients may be explained as due to 1) IBD misdiagnosis which is well-acknowledged in the gastroenterology community, 2) a possible mixed infection as reported recently (9) or 3) a possible need for reclassification of IBD as one disease with two forms as seen in tuberculosis and leprosy (34). With regard to tissue from non-IBD patients, MAP was absent in tissue using FISH.

Despite the need for visible number of MAP in the tissue in order to be visualized by CLSM, the majority of CD tissue contained MAP DNA compared to none in the non-IBD controls. Because of this concern related to the strength of MAP signal detected by FISH and recorded by CLSM in tissue, we employed two rounds of nested PCR on DNA extracts purified directly from same tissue samples. The PCR data clearly confirmed the data obtained by FISH. Further more, nested PCR detected MAP DNA in those samples with weaker MAP presence (83% of CD tissue contained MAP DNA by PCR compared to 67% by FISH). The distribution of MAP in intestinal tissue is not homogenous which me explain the results where some CD tissue samples were positive by FISH and not by PCR or positive in the none-inflamed and not in the inflamed tissue sections despite our effort in performing multiple PCR analysis on different sections of the tissue and by extensive scanning of multiple slides by CSLM when sample size allowed. The data clearly indicate that MAP is present in the majority of CD subjects compared to non-IBD controls thus providing more evidence towards the association of MAP with CD etiology.

CHAPTER THREE: POSSIBLE MYCOBACTERIAL ROLE IN FUNCTIONAL DYSREGULATION OF POLYMORPHONUCLEAR LEUKOCYTES AND PERIPHERAL BLOOD MONONUCLEAR CELLS IN CROHN'S DISEASE

Introduction

Pathogenic mycobacteria actively interfere with the cell-mediated immunity (CMI) of the host probably by dysregulating intracellular signaling pathways that further disrupt the network of cytokine signals that are supposed to organize, direct and modulate the immune response in order to eradicate the invading agent. A genetic predisposition in the host may play a role in how the disease manifests itself. In leprosy, individuals who produce a Th1 biased CMI reaction develop the contained tuberculoid form of leprosy, while those that produce a Th2 oriented CMI response develop the aggressive lepromatous form of the disease (6). Although some evidence of this type of immune-modulation possibly by MAP in CD patients may exist (22), it is unclear as to what role this immune-modulation may take in the etiology of CD. Mycobacterial heat shock proteins (HSP) are of interest due to their homology with human analogues and the enhanced production of antibodies and T cells which recognize mycobacterial HSPs in patients with CD (25, 54). While pathogenic bacteria such as adherent-invasive *E. coli* have been implicated in CD (30), others like MAP have been vigorously debated. The pathogenesis of MAP would be expected to be similar to the pathogenesis of tuberculosis. In fact, intestinal tuberculosis and CD may be clinically indistinguishable. *M. tuberculosis, M. leprae* and MAP

possess similar molecular components in their cell walls such as lipoarabinomannan which suppress antigenic responsiveness of PBL; inhibit antigen presentation; induce production of TNF-alpha; and inhibit IFN-gamma mediated macrophage activation (49). Bacterial lipoproteins via toll-like receptors (42) and IFN-gamma released from primed T-cells (8) and NK cells stimulate macrophages to produce the cytokine IL-12, which further stimulate both primed and naïve Th1 T-cells and also NK cells, inducing the release of TNF. TNF plays an important role in the pathogenesis of CD. Blocking TNF has been shown effective in reducing inflammatory symptoms in moderate to severe CD patients (73). IL-12 has been proposed as a marker of T-cell activation in sarcoidosis (47), and may be important in mediating the T-cell response in CD (69). Patients with tuberculosis often exhibit a negative PPD (purified protein derivative) skin test and a lack of T-cell responsiveness to mycobacterial antigen (anergy). *In vitro* stimulation of T cells with PPD results in the production of IL-10, IFN-gamma, and proliferation in PPD(+) patients, whereas cells from anergic patients produce IL-10 but not IFN-gamma and fail to proliferate in response to PPD. In anergic patients, IL-10-producing T cells are constitutively present. In this chapter, anergic responses as seen in tuberculosis, the role of MAP and the status of the cellular immune response in CD patients is investigated.

Methods and Materials

Patient Selection and Specimen source

A total of 37 subjects consisting of 23 with CD, 3 with UC, and 11 healthy control individuals were included in this study. Table 3 shows the demographic information and type of

specimens obtained from each subject. In order to investigate bacterial infiltration in host tissue, multiple tissue samples in term of inflamed, non-inflamed and lymph nodes from individual subjects were sought and obtained when possible. Over all, a total of 43 surgically resected tissue specimens were obtained and analyzed in this study. Of which, 39 tissue samples (17 inflamed, 15 non-inflamed and 7 lymph nodes) were obtained from 17 CD subjects, and 4 tissue samples (2 inflamed and 1 non-inflamed and 1 lymph nodes) obtained from two UC patients. Full thickness small intestinal and colonic tissue specimens designated by a code were obtained at the time of surgery from consented participating subjects. Informed consent was obtained from each subject in accordance with Internal Review Board (IRB) regulations at the University of Florida and Gainesville VAMC (Veterans Affair Medical Center). Additionally, a total of 31 peripheral blood samples (19 CD, 1 UC, and 11 healthy subjects) were analyzed. A volume of 30 ml of EDTA-whole blood was obtained from each subject when possible and shipped for analysis within 24 hours of collection (76). A survey form with questions concerning family history of IBD, smoking status, ethnic background, fistulizing *versus* non-fistulizing disease, and medications history, especially in the past 4 weeks prior to giving clinical specimens was completed per subject (Table 3).

Tissue Collection and Processing

The tissue samples were catalogued blindly and referred to only by their assigned code. Macroscopic examination of the tissue samples was done immediately following the arrival of the tissue to the laboratory. Tubes containing marked inflamed tissue were processed separately from those marked as non-inflamed, lymph nodes or normal tissue. Each tissue was removed

from the transport tube and sectioned into three parts. One part was processed for genomic DNA extraction followed by PCR analysis, second part was homogenized, decontaminated and processed for culture and the last part was flash frozen in liquid nitrogen.

Peripheral Blood Withdrawal and Processing

Fresh blood samples assigned with a code were immediately processed in a Biosafety Cabinet Class II as follows: PMN and PBMC were isolated using polymorphprep and lymphoprep density gradient separation medium following the manufacturer's procedure (Greiner Bio One, Inc). Initially, blood samples were diluted 1:1 (v/v) with room temperature RPMI culture media (Invitrogen, CA). For PBMC isolation, a volume of 4mL of diluted blood was layered on 4mL Lymphoprep solution in 15mL polypropylene tubes. For PMN isolation, a volume of 5mL of the whole blood-RPMI (Roswell Park Memorial Institute) mixture was layered on 5mL polymorphprep solution in 15mL polypropylene tubes. Tubes were centrifuged at 1,550 rpm and room temperature for 30 m. This results in formation of the density gradient interface, which is followed by isolation of bands containing PBMC or PMN. Purified cells then were transferred into sterile tubes for further use.

Microbial Genomic DNA Extraction and PCR Analysis

The PCR protocol for detection of the MAP IS900 DNA element was adapted from that kindly provided by Dr. J. Hermon-Taylor (St. George's Hospital Medical School, London, U.K.). Five hundred mg of fresh tissue was diced into fine pieces using sterile disposable scalpels. The tissue sample was re-suspended in 4.0ml mycobacterial lysis buffer (2mM EDTA, 400 mM

NaCl, 10 mM TrisHCl pH8, 100 ug/ml Proteinase K, and 0.6% SDS) and homogenized by an Omni Tip disposable generator probe (Fisher Scientific Pittsburgh, PA) for 1 m at 30,000 rpm. The tissue sample was incubated with shaking (200 rpm) at 37°C for 3 h, transferred to disposable FastPrep® lysing matrix B blue cap tube (Qbiogene, Carlsbad, CA), and ribolysed at 6.5m/s^{-2} for 45 s by using a FastPrep® ribolyser (Qbiogene, Carlsbad, CA). The samples are placed on ice immediately for 15 m. The DNA is then isolated by phenol/chloroform/isoamyl alcohol and ethanol precipitation. DNA pellet was dissolved in 250 μL TE buffer. The MAP specific IS900 DNA element was evaluated in triplicate using a nested primer PCR technique. Briefly, oligonucleotide primers P90 (5'-GTT-CGG-GGC-CGT-CGC-TTA-GG-3') and P91 (5'-GAG-GTC-GAT-CGC-CCA-CGT-GA-3') were selected to amplify a unique 398 bp fragment of 5' region of IS900. To reliably detect MAP, AV1(5'-ATG-TGG-TTG-CTG TGT-TGG-ATG-G-3') and AV2(5'-CCG-CCG-CAA-TCA-ACT-CCA-G-3') were used for the nested PCR in the second round using the 398 bp amplified fragment as a template to amplify a 298 bp internal sequence. The PCR reaction mixture consists of 1×PCR buffer, 1.5mM $MgCl_2$, 0.1mM dNTP, 6% DMSO, 2μM primers, and 3.5u/50μl Platinum Taq polymerase (Invitrogen Carlsbad CA). Five μl of DNA template was used in first around PCR reaction in 50μl. A volume of 1μl of PCR product from first round was used in second round PCR in 50μl. The PCR cycling conditions were as follows: 95°C for 5 m, 40cycles of 95°C for 1m, 58°C for 1m, 72°C for 3 m; and a final extension of 5 m at 72°C. The amplification product size was determined on an agarose gel. Some of the nested PCR products were gel purified and sequenced by the University of Florida DNA Sequencing Core facility confirming that the product was identical to the MAP IS900 sequence. Appropriate controls were included and analyzed side by side in every phase of

the experiments. This includes negative controls during genomic DNA extraction and the two rounds of PCR preparations. MAP genomic DNA from a CD clinical isolate was used a positive control. However, the genomic MAP DNA was extracted independently and was analyzed in a separate Biosafety cabinet facility and using different supplies.

In-vitro Phagocytosis Assay

A clinical MAP strain Linda isolated from CD tissue was used in this study. MAP was cultured in 7H9 broth media supplemented with mycobactin J (Allied Monitor). Each MAP preparation of 1 x 10^7 CFU/ml was labeled by incubating with 100ug of FITC (Molecular Probes), for 30 m at room temperature. Following centrifugation at 13,000rpm for 5 m, supernatant was discarded, and labeled MAP cells were washed twice with PBS, pH 7.2. FITC-labeled MAP was then suspended in 100uL of RPMI media. The efficiency of *in vitro* phagocytosis of FITC-labeled MAP by PMN or PBMC was evaluated as follows. In triplicate, tubes with each has 1 x 10^6 of PMN or PBMC from 19 CD patients, 1 UC patient, and 11 healthy control subjects were incubated with 1 x 10^7 CFU of FITC-labeled MAP in the presence of 100uL plasma from corresponding subject for 2 h at 37 ^oC followed by the addition of 100uL of 0.2% trypan blue (Sigma, MO) in order to quench non-specific fluorescence. A volume of 200uL from each sample was aliquoted into a 96-well plate and the absorbance readings were measured at 485nm/535nm. Similar set up consisted of PMN, PBMC and plasma from a standard control was performed side by side with CD and healthy control subjects. The amount of internalized FITC-labeled MAP by cells from tested subjects was then compared to that from the standard control. In order to study presence of plasma inhibitors, crossover experiments were performed

where PMN or PBMC from tested subjects were exposed to FITC-labeled MAP in the presence of 100uL plasma from a standard control and *vice versa*.

Confocal Scanning Laser Microscopy Analysis

Three different bacterial strains were used in this study. A clinical MAP strain Linda isolated from CD tissue, *Mycobacterium tuberculosis* ATCC # 25177 (American Type Culture Collection, VA), and *Escherichia coli* strain TOP10 (Invitrogen, CA). Localization of FITC-labeled viable and dead bacterial cells was investigated in infected PMN by Confocal Scanning Laser Microscope (CSLM). Samples consisting of PMN from CD and control subjects infected *in vitro* with FITC labeled-bacterial cells were spotted on microscopic slides, mounted with antifade and then scanned by Zeiss CSLM. Slides were scanned under 40x objective lenses with oil. All variables, such as photometric gain, photomultipler setting, pixel size, objective size, mounting medium, and numbers of scans to accumulation were recorded for each scan and images were documented.

Cell Proliferation Assay

Initially, the optimum PHA concentration was determined through titration. Aliquots of 1 x 10^5 cells of PBMC from healthy subjects were plated and exposed to serial dilutions of PHA mitogen at final concentrations of 0.019, 0.078, 0.31, 1.25, 5, 20, and 80 ug/mL. The microtiter plates were incubated at 37^{o}C and 5% CO_2 for 72h. PBMC were labeled with bromodeoxyuridine (BrdU, Roche Molecular Biochemicals, IN) and reincubated for additional 24 h, and cell transformation was then measured using cell proliferation ELISA BrdU

commercial kit from Roche (Indianapolis, IN). Briefly, the BrdU incorporation was measured by using a monoclonal antibody, anti-BrdU-POD, conjugated with peroxidase. The immune complexes were detected by a substrate reaction and the reaction product was quantified by measuring the absorbance at 492nm in an ELISA Auto Reader II (Ortho Diagnostic Systems, Inc). Solutions containing optimal concentration of PHA were prepared in sterile RPMI 1640 (Invitrogen, CA). The stocks were dispensed into sterile vials, in suitable volume for one assay, and held frozen at -20^{o}C until use.

Immunoreactivitiy of PBMC derived from CD and healthy subjects were evaluated as follows. In triplicates, PBMC at a final dilution of 1×10^{5} cells/ well in a 96-well microtiter plate were mixed with plasma either from CD or control subjects. Mitogens and antigens investigated in this study included PHA (20ug/mL, Sigma, MO), *Candida albicans* extract (20 ug/mL; Greer Laboratories, NC), pokeweed mitogen (PWM, Sigma, MO) at 10 ug/mL and MAP purified protein derivative (PPD; 5ug/mL). The MAP PPD was prepared in our laboratory by sonication of cell pellets from MAP culture grown to mid-log phase (approximately six weeks) followed by centrifugation at 16,000 rpm for 30 m, Cell debris were discarded and PPD supernatant was transferred to sterile tube and stored at -80 ^{o}C until use. The microtiter plates were incubated at 37^{o}C and 5% CO_2 for 72h. PBMC were labeled with BrdU (Roche Molecular Biochemicals, IN) and reincubated for additional 24 h. Cell transformation was measured *in vitro* using cell proliferation ELISA BrdU commercial kit from Roche (Indianapolis, IN) as described earlier.

Statistical Analysis

Absolute values of one (positive) and zero (negative) were assigned to the observed data for each population and the variance was calculated by using the F-test for variances. Data were normalized by multiplying each datum by the inverse of the variance of its group. To evaluate the significance of the differences between each population we performed one-way ANOVA on the normalized data. Differences with p values < 0.05 were considered significant.

Results

Detection of IS900 Gene of MAP by Nested PCR

Two rounds of nested PCR using IS900-derived oligonucleotide primers were employed on 43 DNA extracts isolated directly from homogenized tissue specimens used in this study. The second round of PCR is considered the key step for the detection of MAP as indicated by the amplification of a 298 bp fragment. Multiple tissue specimens from different part of resectioned intestinal parts on individual subjects especially from CD patients were sought in this study in order to investigate infiltration of the MAP bacterium into the host tissue. Nested PCR detected MAP DNA in 21/43 all tissue samples; 19 CD tissue and 2 UC tissue. MAP infiltration in host tissue was confirmed following the detection of MAP DNA is neighboring non-inflamed and lymph nodes tissue. Specifically, MAP DNA was detected in tissue from 15/17(88%) CD subjects and 1/2(50%) UC patients. As shown in Fig. 6, MAP in 15 CD patients was detected in 9 non-inflamed tissue (Fig. 6A lanes 2, 7, 11, 13, 20 and Fig. 6B lanes 4, 7, 10, 13), in 7 inflamed tissue (Fig.6A lanes 8, 10, 15, 17, 19, 21 and Fig.6B lane 3) and in 4 lymph nodes

tissue (Fig.6A lane 26 and Fig 6B lanes 2, 5, 12). In UC patients, MAP DNA was detected in two tissue samples (Fig. 6B lanes 14 and 15) from 1 out of two patients. Representative of the 298 bp fragments from amplified DNA from MAP positive tissue samples were sequenced. Following blast and alignment analysis of the nucleotide sequence amplified from positive tissue samples confirmed the amplification of the IS900 gene unique to MAP.

Evaluation of PMN and PBMC Phagocytosis Uptake Mechanism

In vitro phagocytosis of FITC-labeled MAP by PMN and PBMC derived from 19 CD patients was investigated and compared to those from 1 UC patient and 11 healthy controls. Initially, it was determined that FITC had no toxicity effect on the viability of MAP following a viability study where FITC-labeled MAP and unlabeled MAP were inoculated into mycobacterial broth culture media; both treatments gave similar growth properties. The efficiency of phagocytic cells from CD patients to uptake and phagocytose viable FITC-labeled MAP was determined by the measurement of internalized fluorescence signal following quenching of unwashed and unphagocytosed FITC-labeled MAP. The uptake of FITC-labeled MAP by subject's PMN or PBMC in the presence of subject's plasma was compared to the uptake of FITC-labeled MAP by PMN or PBMC from a standard normal control in the presence of plasma from the same standard normal control. Consequently, any suppression in phagocytosis uptake can be quantitatively determined. Whether the suppression is due to defect in the cells or to presence of cell-specific plasma inhibitors was determined following the cross over experiments using PMN, PBMC and plasma from a standard normal control. Table 4 summarizes the phagocytosis efficiency of viable MAP by PMN and PBMC and the effect of

possible cell-specific plasma inhibitors from blood samples of 31 subjects used in this study. PMN phagocytosis was suppressed in 13/19 CD subjects (68%) compared to none in controls ($p< 0.001$); suppression ranged from 6 to 97%. PBMC phagocytosis was suppressed only in 5/19 (26%) of CD subjects; suppression ranged between 1 to 70%. Following exposure of similar amount of PMN from CD patients and a standard normal control each to 10^7 CFU of FITC-labeled MAP in the presence of their correspondence plasma, the amount of phagocytosed MAP by PMN is lower in CD patients compared to standard normal control. The quantitative measurement of phagocytosis suppression has been determined for all 31 subjects included in this study (Table 4).

In order to investigate weather the suppression in phagocytosis uptake is due to defect in PMN or PBMC or to presence of cell-specific inhibitors that may interfere in the phagocytosis, a cross over experiment was designed. The subject's cells incubated with FITC-labeled MAP were tested in the presence of standard control plasma. Accordingly, the uptake value for each cell type may remain similar if cell-specific plasma inhibitors are absent; the opposite is also true. As shown in Table 4, PMN-specific plasma inhibitors were detected in 9/19 (47%) CD subjects compared to none in controls ($P<0.05$). The negative effect of the presence of PMN-specific inhibitors in plasma from CD patients on healthy PMN phagocytosis has also been measured which ranged between 2 to 67% (Table 4). Plasma inhibitors specific to PBMC phagocytosis were mildly present in CD patients; present only in 3/19 (16%) CD subjects compared to none in controls. All 13 (68%) CD subjects that have suppressed PMN phagocytosis were also positive for MAP DNA detection in tissue.

The localization of internalized viable and dead bacteria is graphically illustrated in figures 7, 8, 9 and 10 corresponding to phagocytosis by PMN from healthy, UC, and CD subjects respectively. Viable and dead *E. coli* (Fig. 7A, 7B, 8A, 8B, 9A, 9B, 10A) and *M. tuberculosis* (Fig. 7C, 7D, 8C, 8D, and 9D) as well as dead MAP (Fig. 7F, 8F, 9F) localized similarly throughout the cytoplasm of PMN from all 3 different subjects. In contrast, viable *M. tuberculosis* and viable MAP localized closer to the cytoplasmic membrane in phagosomes inside PMN isolated only from CD patients (Fig. 9C, 9E, 10B, 10C), but not from healthy (Fig. 7C and 7E) or UC (Fig.8C and 8E) cells.

T-Lymphocyte Proliferation

The use of PHA, which is a plant mitogen, has been proven to be useful in investigating and assessing the overall function of lymphocyte responsiveness. PHA stimulates lymphocytes directly by mechanisms different than those used for specific antigen processing and presentation to lymphocytes. In this study, a final concentration of 20 ug/mL PHA mitogen following 72 h of incubation has been identified to provide optimum lymphocyte activation. Therefore, all experiments including PHA were performed at this PHA concentration.

In addition to PHA, the mitogen PWM and extracts from *C. albicans* and PPD from MAP were used to investigate the proliferative response of T-lymphocytes and its interaction with neighboring relevant cells such as B-lymphocytes and antigen presenting or other dendritric cells. The proliferative response of PBMC isolated from CD and healthy control patients was quantitatively measured and compared to that of PBMC isolated from a standard normal control. Normal proliferative response was reported when PBMC from tested subjects matched or reacted

better than those from a standard normal control. Inactive proliferative response was reported when PBMC from tested subjects failed to react similarly to the standard normal control. As shown in table 5, PBMC from 8/19 (42%) CD subjects showed dysfunctional proliferative response against PHA (ranged between 1 to 82%) compared to 1 in controls suggesting possible T-cell anergy. More over, PBMC from 3 of these 8 CD subjects, reacted negatively against *C. albicans* extract suggesting a possible defect in antigen recall ability by activated monocytes. PBMC from the UC patient reacted normally to PHA and slightly to MAP PPD suggesting environmental mycobacterial exposure. PBMC from the 11 CD subjects that reacted normally to PHA, 7 reacted strongly to MAP PPD suggesting pre-exposure to *Mycobacteria*, one reacted mildly to MAP PPD suggesting possible cross reactivity with environmental mycobacterial antigens and 3 did not react with MAP PPD suggesting lack of mycobacteria pre-exposure. Of 11 healthy control subjects, 10 (91%) reacted normally to PHA. Mild reactivity to MAP PPD due to cross reactivity with environmental mycobacterial antigens was detected in 2 healthy control subjects. PWM provided limited information in this study. Over all 15 out of 19 (78%) CD subjects either indicated possible T-cell anergy or MAP pre-exposure compared to detection of MAP DNA in tissue from 15/17 (88%) CD subjects.

Discussion

In this study MAP was used to evaluate the phagocytic function of PMN obtained from CD and UC patients undergoing bowel resections. The results shown in Table 4 reveal a significant decrease in the uptake of FITC-labeled MAP by PMN from CD subjects compared to those from controls. This may suggest an original defect in the innate immune response of CD

patients or it may reflect an acquired, secondary defect in the immune response caused by the disease itself. Both possibilities may co-exist, especially if a genetic trait predisposes to an infection with an etiologic microbe. Other pathogenic bacteria such as members of *Brucella* are known to interfere with phagosome/endosome trafficking as a survival strategy to avoid immune destruction. This observation is similar to events that occur in *M. tuberculosis*-infected immune cells where the pathogen interferes with signals and dysregulates the immune system so that an effective response is not initiated. Geijtenbeek et. al (28) demonstrated that *M. tuberculosi*s binds to DC-SIGN (dendritric cell-specific intracellular adhesion molecules, ICAM, intracellular adhesion molecules) to interfere with DC maturation and signaling that further dysregulates T-cell function and results in an ineffective cell mediated immune response against the bacterium. The immature DC's are still able to present MHC-antigens but lack the required co-stimulatory molecules needed to cause a robust and properly coordinated Th1 response.

In this study, Figures 9E and 10C demonstrated that viable MAP was localized near the inner side of the cytoplasmic membrane away from the center of the cytoplasm of an *in vitro* infected PMN from CD patients. This correlates with viable *M. tuberculosis* (Fig. 9C and 10B) where there is a visible phagocytic vacuole containing bacteria protruding from the cell membrane. We did not observe the same pattern with cells from either the healthy or UC controls where bacteria localized throughout the cytoplasm indicating that is being processed and destroyed by the immune system of these individuals. This finding suggests that CD results from a complex interplay of factors including the genetic make-up of the host. As polymorphisms within the NOD2 gene have been associated with increased CD susceptibility (68), other undiscovered genes may be responsible for a genetic defect in PMN phagocytosis of CD

patients. This finding is similar to the facts discussed earlier regarding host-agent interaction reported in Brucellosis and tuberculosis diseases. This data graphically confirm an earlier report which proposed that MAP resists intracellular killing by residing within a phagosomal compartment that retains the characteristics of early phagosomes and resists maturation into functional phagolysosomes (48).

In lymphocytes derived cells from CD patients, transformation responses to some antigens assess their degree of prior sensitization. Since mitogens directly stimulate lymphocytes by bypassing macrophage presentation, decreased mitogen stimulation (PHA) indicated a global non-reactivity in the patient's lymphocytes. But anergy is usually associated with a specific antigen, so it is expected to be observed as a decreased response to a specific antigen. As shown in Table 5, we observed T-cell anergy due to failure to respond normally to PHA in 8 out of the 19 CD subjects. We also observed strong reactivity to PPD from MAP in 7 out of 11 CD subjects who responded normally to PHA. The observation of T-cell anergy in blood samples from significant CD cases compared to none in healthy control and the fact that T-cell from CD patients have shown to be presensitized to MAP clearly suggest a possible MAP involvement in some CD cases. These findings are so similar to immunological events occur in tuberculosis.

The data presented shows a possible role of MAP in CD pathogenesis and may be helpful toward choosing the appropriate treatment protocol for this complex disease by knowing the status of the immune response in CD patients.

CHAPTER FOUR: ANALYSIS OF GENE EXPRESSION IN BUFFY COATS FROM CROHN'S DISEASE PATIENTS

Introduction

DNA microarray technology has become the most widely used technique for global expression studies. Since the first microarray experiment was described (75), it has provided an unprecedented opportunity to generate gene expression data on a genomic scale. Medical application of microarray technology is very limited since gene expression varies normally. A study done by Whitney et al. provides a strong support for the feasibility of using gene expression patterns in peripheral blood as a basis for detection and diagnosis of disease in human patients. They showed that the degree of variation in gene expression in the blood of healthy individuals is smaller than the one seen in the individuals who had cancer or infection (81). In this chapter, we used microarray technology to identify the expression profile of genes to be involved that are required, or have a role in the immune response of CD patients.

Methods and Materials

Patient Selection and Specimen Source

A total of 11 subjects consisting of 8 healthy controls, 2 CD and 1 UC patients were included in this study. Informed consent was obtained from the subjects in accordance with

Institutional Review Board regulations at the University of Florida, Gainesville VAMC, and the University of Central Florida. The diagnosis of CD or UC was established on standard clinical, endoscopic, histologic, and radiographic criteria (7). One whole blood sample drawn into a K_2-EDTA sterile vacutainer® tube was collected from each subject. All samples were coded and a self-reported health status and medication use of each subject was recorded using a standardized questionnaire in order to minimize variables such as age, gender, and medication interference.

Peripheral Blood Withdrawal and Processing

The samples were immediately processed in a class II biosafety cabinet. For buffy coat extraction, the tubes were centrifuged at 3000 rpm for 10 min. The buffy coat layer from each tube was transferred into a RNase-free tube containing 800 uL of RNA later solution (Ambion, CA) and kept refrigerated until processing.

Microarray Analysis

The protocols used for this study were obtained from those developed for the analysis of human microarrays (38).

Array Chip:

A 30,000-gene clone set made of PCR-amplified cDNA clones that represent unique human transcripts within the Expressed Sequence Taq (EST) from UniGene (http://www.ncbi.nlm.nih.gov/UniGene/) at the National Center for Biotechnology Information and The Institute for Genomic Research (TIGR) Human Gene Index (HGI)

(http://www.tigr.org/tigr-scripts/tgi/T_index.cgi?species=human). The TIGR protocol assembles the ESTs within clusters to produce tentative human consensus (THC) sequences. Purified PCR-amplified genes were arrayed by using the Molecular Dynamics Generation III Array Spotter. This arrayer deposits nanoliter volumes of samples at high density onto aminosilane coated glass slides.

Total RNA Isolation:

Total RNA was extracted from freshly isolated buffy coats, PMN and PBMC by using a modified protocol from the RNAqueous –4PCR kit (Ambion, CA).

RNA labeling and hybridization:

Total RNA was used as a template for random-primed first-strand cDNA synthesis in the presence of amino-allyl-dUTP (Sigma, MO) during reverse transcription, then the purified products were conjugated to fluorescent dyes. A pooled of total RNA extracted from the 8 healthy individuals was used as a reference RNA sample to provide a common internal reference standard for comparison. Hybridization reactions were conducted as described in The Institute for Genomic Research (TIGR) standard operating procedures (http://www.tigr.org/tdb/microarray/protocolsTIGR.shtml).

Data Collection:

Hybridized slides were scanned using the Axon GenePix 4000 microarray scanner, and the independent TIFF images from each channel were analyzed using TIGR Spotfinder

(http://www.tigr.org/software/tm4/spotfinder.html) to assess relative expression levels. Spots with lower intensity than local background were assigned 0 values. Spots with intensities less than 1.5 times the local background level in either of the two channels were eliminated before data normalization to remove unreliable low-intensity spots.

Data Normalization and Data Analysis:

Normalization is necessary to adjust for differences in labeling and detection efficiencies of the fluorescent labels and for differences in the quantity of starting RNA. Data was normalized using a local regression technique, LOWESS (Locally Weighted Scatterplot Smoothing), using the MIDAS software tool (http://www.tigr.org/softlab, TIGR). All calculated gene expression ratios were $\log_2$-transformed, and differentially expressed genes at the 95% confidence level for each reference set were determined by assuming the $\log_2$ ratios for each data set form a normal distribution, and selecting genes with $\log_2$ (ratio) values > 1.96 standard deviations from the mean (2). This filtration of the significantly expressed genes was conducted using MIDAS, and the resulting lists of the genes were examined further by cross comparison between experiments using TIGR MeV (http://www.tigr.org/softlab, TIGR) with EASE (Expression Analysis Systematic Explorer), which allows the biological interpretation of gene clusters.

Results

To explore and characterize the gene expression profiling within CD and UC disorders, 3 total RNA samples from 1 UC and 2 CD patients, were analyzed against a reference sample of

pooled total RNA from 8 healthy individuals. Samples were analyzed by comparative hybridization to DNA microarrays containing 30,000 elements representing unique human transcripts.

We found that 17% (5630 genes) of the total number of genes was differentially expressed in both IBD disorders compared to the reference pooled sample. These genes were distributed mainly within four biological themes (Fig. 11) classified as cellular processes (38%), physiological processes (26%), intracellular genes (18%), and genes involved in metabolism (18%). We focused our investigation primarily on genes directly related to the immune response since CD and UC are complex diseases characterized for chronic intestinal inflammation. Of the 5630 genes differentially expressed in the experimental samples, 238 genes belonged to genes involved in the immune response (Fig.12).

As shown in Table 6, seven genes where common to both forms of IBD with variation in the level of gene expression where 6 genes were downregulated and 1 gene was upregulated. Two downregulated genes corresponded to the same biological description (GenBank numbers W79396 and AI262976). These 2 genes contain a C2h2 zinc finger and belong to one of the largest gene families in the human genome. These proteins are involved in transcriptional regulation and are quite conserved throughout evolution (2). Another downregulated gene was the NKG2E (GenBank number W93370) that plays a role as a receptor for the recognition of MHC class I molecules by NK cells and some cytotoxic T-cells (31). The CD160 antigen precursor (GenBank number AA463248) was also found to be downregulated (1). The expression of the Secreted phosphoprotein 1 (GenBank number AA775616) was downregulated. This protein acts as a cytokine involved in enhancing production of interferon-gamma and

interleukin-12 and reducing production of interleukin-10 and is essential in the pathway that leads to type I immunity (50). Carbohydrate sulfotransferase 2 or CHST2 (GenBank number AA682637) is a Golgi membrane-bound sulfotransferase that catalyzes the transfer of sulfate to position 6 of a N-acetylglucosamine (GlcNAc) residue. Its mouse homolog has been involved in the biosynthesis of 6-sulfosialyl Lewis X antigen, which is a component of L-selectin ligands (51). The only upregulated gene between UC and CD samples was the Toll-like receptor 4 precursor (GenBank number AI371874), which is highly expressed in PBL and mediates the innate immune response to bacterial lipopolysaccharide (LPS) (56).

Eight genes were found to be either upregulated or downregulated in CD or UC only (Table 7). Within the unique genes, we found a protein encoded by the gene TRIM22 (GenBank number AA083407), which is induced by interferon and it has been involved in the mediation of interferon's antiviral effects (79). The expression of the small inducible cytokine A18 precursor (CCL18) or macrophage inflammatory protein (MIP-4) was upregulated in UC patients, and downregulated in CD patients. This cytokine is a chemotactic factor that attracts naive T lymphocytes toward dendritic cells and activated macrophages in lymph nodes, but not monocytes or granulocytes (41). Interestingly, another gene with similar function to CCL18, Lymphotactin precursor (XCL1) (GenBank number AI298976), was also found to be downregulated in CD patients only. A gene that codes for an integral membrane protein which is a probable mediator of viral effects on B lymphocytes (GenBank number AI123732) was found to be downregulated in CD patients. This gene is predicted to encode a G protein-coupled receptor. Expression of this gene was detected in B-lymphocyte cell lines, but not in T-lymphocyte cell lines. The function of this gene is unknown (4). The expression of the small

inducible cytokine A3 precursor (CCL3) or Macrophage inflammatory protein 1-alpha (MIP-1-alpha) (GenBank number R47893) was downregulated in CD patients. This cytokine is one of the major HIV-suppressive factors produced by CD8+ T cells (13). Lymphotoxin-beta receptor (GenBank number AA454646) is a member of the tumor necrosis factor (TNF) family of receptors. Activation of this protein can trigger apoptosis (84). We found of great significance the differential expression of the gene that codes for IFNGR1 since defects in this gene have been directly linked to susceptibility to mycobacterial infection (15, 44, 45). The expression of this gene was downregulated in CD patients only.

Discussion

Previous studies showed that large ZAS proteins with two separate C2H2 zinc finger pairs, independently bind to specific DNA sequences, including the kappaB motif. These proteins associate with a TNF receptor- factor to inhibit NF-kappaB- and JNK/ SAPK-mediated signaling of TNF-alpha (83). This might explain why TNF-alpha plays an important role in CD pathology. Since its regulation is altered, the TNF-alpha signaling pathways are constantly active increasing the inflammation process in CD patients. Natural killer cells are being found to play a primary role in preventing and removing cancer cells in the body, and removing many types of viruses (31). CD160 antigen is specific for NK cells and its expression was also downregulated, adding to a possible defective NK cells function. This may be linked to the secondary viral infections that few IBD patients develop.

In a previous study, a mouse cDNA encoding GlcNAc-6-O-sulfotransferase was cloned and was identified as homolog of the human CHST2. When expressed in mammalian cells, the

mouse protein exhibited GlcNAc-6-O-sulfotransferase activity and was involved in the biosynthesis of 6-sulfosialyl Lewis X antigen, which is a component of L-selectin ligands. The L-selectin system is implicated in inflammatory leukocyte trafficking in both acute and chronic settings. By blocking 6-sulfosialyl Lewis X antigen in human lymphoid organs, the L-selectin dependent adherence of lymphocytes to high endothelial venules (HEV) is affected (70). If human CHST2 has a similar function as its mouse homolog, one can speculate that the process of recirculation of lymphocytes from the blood into lymphoid organs ("homing") and back to the blood could be affected in these patients.

It is interesting to find upregulation in the expression of TLR4 indicating the presence of bacterial LPS in both disorders. TLR4 acts via TRAF6 in the activation of NF-kappa-B, cytokine secretion and the inflammatory processes frequently observed in these patients. The fact that the expression of the Staf-50 or TRIM22 encoded protein was downregulated in UC patients only suggests that these patients may be more vulnerable to a secondary viral infection than CD patients.

The expression of CCL18 or MIP-4 and Lymphotactin precursor (XCL1) was downregulated only in CD patients. This may add to the ineffective process of antigen presentation in CD, but not in UC. A study showed that the lymphotoxin-beta receptor mediates cell death in HeLa cells (84). The gene that encodes this protein was upregulated in UC patients only, which might explain the reduced number of immune cells in tissue lesions compared to the ones seen in CD.

IFNGR1 encodes the ligand-binding chain (alpha) of the IFN-gamma receptor. It is known that defects in IFNGR1 are a cause of familial disseminated atypical mycobacterial

infection and disseminated bcg infection. Patients suffering from this deficiency have an immunologic defect predisposing them to infection with mycobacteria (15, 44, 45). Surprisingly, we found downregulation of IFNGR1 only in CD samples, but not in UC samples. This correlates with the proposed theory as *Mycobacterium avium* subspecies *paratuberculosis* (MAP) being the causative agent of CD (11, 40, 53, 62).

In summary, we used cells from a simple human tissue (blood) to investigate the variation in gene expression within two human disorders. This work supports the establishment of two different IBD disorders with different etiological processes and strengthens the mycobacterial etiology of CD.

CHAPTER FIVE: GENERAL DISCUSSION

Investigating the association of MAP or other agents in CD etiology remains a source of a major debate among investigators. The data reported by those supporting the association of MAP with CD etiology is credible and their argument has merit. However, it is also responsible to keep an objectivity regarding other studies, which reported the possible involvement of other factors in the etiology of Crohn's syndrome. Variation in the selection and use of methodology is the underlining cause for the mixed outcome in these studies. The debate may vary with regards to the percentage of CD cases associated with MAP. Attempts to culture MAP from tissue samples from CD patients have been tried in the past. The outcome depended significantly on the technology used and the specimen selection and processing. In our laboratory we reported previously the isolation of MAP from full-thickness tissue samples obtained from CD patients following short term incubation in mycobacterial growth indicator tube (MGIT) culture media (76). Using the same culture media, we isolated MAP from breast milk from two CD lactating mothers (62). In both reports, IS900-based PCR was employed to verify MAP presence in the culture. This was recently confirmed in Hermon-Taylor laboratory where 92% of intestinal biopsies were positive for MAP compared to 26% in controls (7). The nature of MAP in CD tissue is significantly different from those in animals with JD (64). Therefore, using technology designed for isolation of bacillary form of MAP as in JD sources may not be applicable to that in human with CD. That alone will play a major factor in the outcome of the study. There is a

possibility that exposure to MAP could occur through environmental fecal contamination or from the milk or blood from JD-infected animals (32, 78).

Phagocytosis is an extremely important process for the recognition, ingestion, and digestion of antigen(s) in the host defense mechanism. As described by Hornef *et al*., there are several mechanisms that bacteria use as a defense against phagocytes (42). These include apoptosis, inhibition of antigen uptake, bacterial escape from the endosome, interference with the maturation of the immune cells and/or their phagosomes, and subcellular localization of defense factors. It is worth mentioning the mechanisms by which a well-known intracellular pathogen, *Mycobacterium tuberculosis*, suppresses antigen presentation and T-cell activation. *M. tuberculosis* inhibits phagosomal maturation by depleting H^+ ATPase molecules from the vacuolar membrane. This leads to reduced acidification and allows intracellular survival and growth. This correlates with a combination of inadequate clearance of MAP by PMN from CD patients and impaired macrophage function as shown in this study.

For many years immunosuppressants and/or antibiotics were used to treat CD (27). Given the historical confusion over the etiology and pathogenesis of the syndrome, the approach for treating the disease by suppressing inflammatory symptoms with immunosuppressants can be regarded as random at best – and at worse – detrimental. Most therapeutic strategies have tried to suppress the overactive adaptive immune response. The use of random, single agent antibiotic regimens used in the past may or may not have been helpful. Recently, another approach has been proposed that is based on the stimulation of the innate immune system with growth factors (19, 21). GM-CSF was administered to 15 CD patients. Twelve patients showed a decrease in the CD activity index, and 8 achieved clinical remission. This suggests that the problem in CD

does not lie in an excessive immune response against self-antigens as argued by the autoimmune theory. On the contrary, it suggests that one major factor involved in CD is an immune deficiency, either primary or secondary or both. CD may be related to the inability of the immune system to defend against a microbial attack and once the mycobacterial infection is established, further insults to the immune system caused by the infection itself exacerbate the problem.

The downregulation in the expression of the IFNGR1 in CD patients only is a strong link to the proposed mycobaterial etiology of Crohn's disease. It also supports why UC patients having MAP exposure don't develop the same clinical manifestations as CD patients or don't respond to anti-mycobacterial treatments.

In a chronic disease such as Crohn's disease, the clinical status and prognosis of the disease depends on the balance between host factors and the pathogenicity of the bacterium. MAP may cause disease by its ability to resist intracellular killing by macrophages and multiply within macrophages. Furthermore, the ongoing immune processes are influenced by parameters such as the immunological status, genetic makeup, and the environment of the host. Taken all together, the data presented in this work adds more evidence towards the association of MAP with CD etiology. It is important to know that in order to understand the problem in its proper perspective, it is essential to take into account the immunological responses of the host and the ways and means by which MAP overcomes the host immune response.

APPENDIX A: TABLES

Table 1: Demographic Information and Type of Specimens used in Chapter Two

SUBJECT			DISEASE					TISSUE SPECIMEN	
SEX	AGE	DIAGNOSIS[a]	SITE[b]	DURATION	TYPE[c]	SURGERIES	IMMUNOSUPRESSION	INFLAMED[d]	NON-INFLAMED
F	25	CD	Colon	4y	F	2	6MP	X	X
M	26	CD	Small Bowel	9y	I	1	Steroids	X	X
F	68	CD	Bowel-Colon	42y	F+S	3	None	X	X
F	56	CD	Bowel-Colon	11y	S	1	6MP	X	X
NA	NA	CD	Small Bowel	20y	S	1	Steroids	X	X
M	60	CD	Colon	5y	I	0	Steroids	X	X
M	43	CD	Small Bowel	14y	I+F+S	1	Steroids	X	X
F	39	CD	NA	19y	I+F+S	3	Steroids, Infliximab	X	X
F	54	CD	Bowel-Colon	4y	S	2	Steroids, 6MP	X	X
M	21	CD	Small Bowel	12y	S	1	Steroids	X	X
M	25	CD	Bowel-Colon	8y	F+S	2	Steroids, 6MP	X	X
F	40	CD	Bowel-Colon	1y	S	1	Steroids, Infliximab	X	NA
M	54	UC	NA	NA	NA	1	None	X	NA
M	42	UC	NA	NA	NA	1	None	X	NA
F	79	non-IBD	NA	NA	NA	1	None	NA	X
NA	NA	non -IBD	NA	NA	NA	1	None	NA	X
M	64	non-IBD	NA	NA	NA	1	None	NA	X
M	73	non-IBD	NA	NA	NA	2	None	NA	X
F	76	non-IBD	NA	NA	NA	1	None	NA	X
M	71	non-IBD	NA	NA	NA	1	None	NA	X

[a]CD = Crohn's disease; UC = Ulcerative colitis; non-IBD = non-inflammatory bowel disease subjects

M= male; F = female; 6MP = 6-mercaptopurine; [b]NA = not available

[c]S = stricturing state; F = fistulizing state; I = inflammatory state

[d]X = Tissue specimen available

Table 2: Detection of MAP DNA in tissue by FISH using CSLM and nested PCR

Code	Diagnosis	Inflamed Tissue		Non-Inflamed Tissue		Either Tissue	
		FISH	PCR	FISH	PCR	FISH	PCR
R2	CD	Positive	Negative	Positive	Negative	Positive	Negative
R7	CD	Positive	Positive	Positive	Positive	Positive	Positive
R8	CD	Positive	Positive	Positive	Negative	Positive	Positive
R13	CD	Negative	Negative	Positive	Positive	Positive	Positive
R14	CD	Positive	Negative	Negative	Positive	Positive	Positive
R15	CD	Negative	Positive	Negative	Negative	Negative	Positive
R19	CD	Negative	Positive	Negative	Positive	Negative	Positive
R20	CD	Positive	Positive	Negative	Negative	Positive	Positive
R21	CD	Negative	Negative	Negative	Negative	Negative	Negative
R24	CD	Positive	Positive	Negative	Positive	Positive	Positive
R28	CD	Negative	Negative	Negative	Positive	Negative	Positive
R35	CD	Positive	Positive	NA	NA	Positive	Positive
Total	12	7/12(58%)	7/12(58%)	4/11(36%)	6/11(55%)	8(67%)	10(83%)
R11	UC	NA	Positive	NA	NA	NA	NA
R25	UC	NA	Positive	NA	NA	NA	NA
Total	2		2(100%)	NA	NA	NA	2(100%)
R3	non- IBD	NA	NA	Negative	Positive	Negative	Positive
R5	non- IBD	NA	NA	Negative	Negative	Negative	Negative
R10	non- IBD	NA	NA	Negative	Negative	Negative	Negative
R16	non- IBD	NA	NA	Negative	Negative	Negative	Negative
R18	non- IBD	NA	NA	Negative	Negative	Negative	Negative
R30	non- IBD	NA	NA	Negative	Negative	Negative	Negative
Total	6			0(0%)	1(17%)	0(0%)	1(17%)

CD: Crohn's disease; UC: ulcerative colitis, NA: not available, Non-IBD: non-inflammatory bowel disease

Table 3: Demographic Information and Type of Specimens used in Chapter Three

Subject			Disease				Specimen			
Code	Sex	Age	Diagnosis[a]	Site[b]	Duration	Type[c]	Inflamed Tissue[b]	Non-Inflamed Tissue[b]	Lymph Node[b]	Blood[b]
R1	M	50	CD	Bowel-colon	7y	S	X	X	NA	NA
R2	F	25	CD	Colon	4y	F	X	X	X	X
R4	M	29	CD	Bowel-colon	16y	I	NA	NA	NA	X
R7	M	26	CD	Small bowel	9y	I	X	X	NA	X
R8	F	68	CD	Bowel-colon	42y	F+S	X	X	NA	X
R9	M	39	CD	NA	NA	S	NA	NA	NA	X
R1 3	F	56	CD	Bowel-colon	11y	S	X	X	NA	X
R1 4	NA	NA	CD	Small bowel	20y	S	X	X	X	X
R1 5	M	60	CD	Colon	5yr	I	X	X	NA	X
R1 7	M	NA	CD	Bowel-colon	11y	S	X	X	NA	X
R1 9	M	43	CD	Small bowel	14y	I+F+S	X	X	NA	NA
R20	F	39	CD	NA	19y	I+F+S	X	X	NA	X
R21	F	54	CD	Bowel-colon	4y	S	X	X	NA	X
R22	F	31	CD	Colon	25y	I	X	X	X	NA
R23	F	21	CD	Bowel-colon	8y	S	X	NA	X	NA
R24	M	21	CD	Small bowel	12y	S	X	X	X	X
R27	M	40	CD	Bowel-colon	14y	S	X	X	X	X
R28	M	25	CD	Bowel-colon	8y	F+S	X	X	NA	X
R34	F	22	CD	Bowel-colon	3y	I+F+S	NA	NA	NA	X
R35	F	40	CD	Bowel-colon	1y	S	X	NA	X	X
R37	F	50	CD	Bowel-colon	10y	I+F+S	NA	NA	NA	X
R38	F	37	CD	NA	NA	NA	NA	NA	NA	X

Subject				Disease			Specimen			
Code	Sex	Age	Diagnosis[a]	Site[b]	Duration	Type[c]	Inflamed Tissue[b]	Non-Inflamed Tissue[b]	Lymph Node[b]	Blood[b]
R39	M	36	CD	Colon	12y	S	NA	NA	NA	X
C1	M	40	Healthy	NA	NA	NA	NA	NA	NA	X
C2	F	28	Healthy	NA	NA	NA	NA	NA	NA	X
C3	M	30	Healthy	NA	NA	NA	NA	NA	NA	X
C4	F	30	Healthy	NA	NA	NA	NA	NA	NA	X
C5	M	46	Healthy	NA	NA	NA	NA	NA	NA	X
C6	M	32	Healthy	NA	NA	NA	NA	NA	NA	X
C7	F	29	Healthy	NA	NA	NA	NA	NA	NA	X
C8	M	31	Healthy	NA	NA	NA	NA	NA	NA	X
C9	M	26	Healthy	NA	NA	NA	NA	NA	NA	X
C10	F	24	Healthy	NA	NA	NA	NA	NA	NA	X
C11	F	27	Healthy	NA	NA	NA	NA	NA	NA	X
R11	M	64	UC	NA	NA	NA	X	X	NA	NA
R25	M	42	UC	NA	NA	NA	X	NA	X	NA
R62	F	41	UC	NA	NA	NA	NA	NA	NA	X

a-CD:Crohn’s disease, UC: Ulcerative colitis, Healthy subjects

b-NA: not applicable or not available, X: specimen available

c-S: structuring state, F: fistulizing state, I: inflammatory state

Table 4: *In Vitro* Evaluation of Phagocytic Uptake of MAP by PMN and PBMC

Code	Diagnosis	PMN Phagocytosis of FITC-MAP		PBMC Phagocytosis of FITC-MAP	
		Uptake[a]	Plasma Inhibitors[b]	Uptake	Plasma Inhibitors
R2	CD	Suppressed (-23%)	Absent	Suppressed (-6%)	Absent
R4	CD	Normal	Absent	Suppressed (-13%)	Absent
R7	CD	Suppressed (-21%)	Present (-27%)	Normal	Absent
R8	CD	Suppressed (-24%)	Present (-2%)	Normal	Absent
R9	CD	Suppressed (-9%)	Absent	Normal	Absent
R13	CD	Suppressed (-35%)	Absent	Suppressed (-1%)	Absent
R14	CD	Suppressed (-7%)	Present (-2%)	Normal	Absent
R15	CD	Normal	Present (-7%)	Normal	Absent
R17	CD	Normal	Absent	Normal	Absent
R20	CD	Suppressed (-97%)	Present (-49%)	Normal	Absent
R21	CD	Suppressed (-42%)	Absent	Normal	Absent
R24	CD	Suppressed (-6%)	Present (-47%)	Normal	Absent
R27	CD	Suppressed (-32%)	Present (-13%)	Normal	Absent
R28	CD	Suppressed (-56%)	Present (-10%)	Suppressed (-70%)	Present (-23%)
R34	CD	Normal	Absent	Normal	Absent
R35	CD	Suppressed (-79%)	Present (-67%)	Normal	Present (-16%)
R37	CD	Normal	Absent	Normal	Absent
R38	CD	Normal	Absent	Normal	Absnet
R39	CD	Suppressed (-11%)	Absent	Suppressed (-12%)	Present (-5%)
C1	Healthy	Normal	Absent	Normal	Absent

Code	Diagnosis	PMN Phagocytosis of FITC-MAP		PBMC Phagocytosis of FITC-MAP	
		Uptake[a]	Plasma Inhibitors[b]	Uptake	Plasma Inhibitors
C2	Healthy	Normal	Absent	Normal	Absent
C3	Healthy	Normal	Absent	Normal	Absent
C4	Healthy	Normal	Absent	Normal	Absent
C5	Healthy	Normal	Absent	Normal	Absent
C6	Healthy	Normal	Absent	Normal	Absent
C7	Healthy	Normal	Absent	Normal	Absent
C8	Healthy	Normal	Absent	Normal	Absent
C9	Healthy	Normal	Absent	Normal	Absent
C10	Healthy	Normal	Absent	Normal	Absent
C11	Healthy	Normal	Absent	Normal	Absent
R62	UC	Normal	Absent	Normal	Absent

a-Phagocytosis uptake was evaluated by exposing subject's PMN and PBMC to FITC-labeled MAP in the presence of plasma from the subject compared to a standard healthy control. Percentage of suppression was reported when phagocytosis uptake by subject's cells was lower than that of the standard healthy control.

b-Plasma inhibitors specific for PMN or PBMC phagocytosis were measured by cross-over experiments incubating the plasma from each subject with cells from the standard healthy control and FITC-labeled MAP. These values were compared to those corresponding to the standard healthy control in the presence of plasma without inhibitors.

Table 5: Evaluation of PBMC Proliferative Response

Code	Diagnosis[a]	PHA[b]	*Candida albicans*[c]	PWM[d]	MAP PPD[e]
R2	CD	Inactive (-1%)	Normal	Normal	No response
R4	CD	Normal	Normal	Normal	Strong
R7	CD	Inactive (-26%)	Inactive (-5%)	Normal	No response
R8	CD	Inactive (-82%)	Normal	Inactive (-27%)	No response
R9	CD	Inactive (-3%)	Inactive (-27%)	Normal	No response
R13	CD	Normal	Normal	Normal	No response
R14	CD	Normal	Normal	Normal	No response
R15	CD	Normal	Normal	Normal	Strong
R17	CD	Inactive (-3%)	Inactive (-2%)	Normal	No response
R20	CD	Normal	Inactive (-19%)	Normal	Strong
R21	CD	Inactive (-4%)	Normal	Normal	No response
R24	CD	Normal	Inactive (-8%)	Inactive (-11%)	No response
R27	CD	Normal	Normal	Normal	Strong
R28	CD	Normal	Normal	Normal	Mild
R34	CD	Normal	Normal	Normal	Strong
R35	CD	Inactive (-2%)	Normal	Normal	No response
R37	CD	Normal	Normal	Normal	Strong
R38	CD	Inactive (-6%)	Normal	Normal	No response
R39	CD	Normal	Normal	Normal	Strong
C1	Healthy	Normal	Normal	Normal	Mild
C2	Healthy	Inactive (-2%)	Normal	Inactive (-14%)	No response
C3	Healthy	Normal	Incative (-13%)	Normal	No response
C4	Healthy	Normal	Incative (-7%)	Normal	Mild
C5	Healthy	Normal	Incative (-10%)	Normal	No response

Code	Diagnosis[a]	PHA[b]	*Candida albicans*[c]	PWM[d]	MAP PPD[e]
C6	Healthy	Normal	Normal	Normal	No response
C7	Healthy	Normal	Normal	Normal	No response
C8	Healthy	Normal	Normal	Normal	No response
C9	Healthy	Normal	Normal	Normal	No response
C10	Healthy	Normal	Normal	Normal	No response
C11	Healthy	Normal	Normal	Normal	No response
R62	UC	Normal	Normal	Normal	Mild

a-CD: Crohn's disease, UC: Ulcerative colitis

b-PHA: Phytohemagglutinin to assess the overall function of lymphocyte responsiveness

c-Candida albicans: Cell extract used to assess the ability of antigen presenting cells to recall antigens

d-PWM: Pokeweed mitogen to assess B cell responsiveness dependent on T-cell activation

e-MAP PPD: Purified protein derivative from MAP to assess previous subject's exposure to the bacterium

Negative values indicate a decrease in subject's cell proliferation compared to those from a standard healthy control

Table 6: Differentially Expressed Genes Common for both IBD Disorders

GenBank	Description	Expression
W79396	Zinc finger protein 211	Downregulated
AI262976	Zinc finger protein 211	Downregulated
W93370	NKG2-E type II integral membrane protein	Downregulated
AA463248	CD160 antigen precursor	Downregulated
AA775616	Secreted phosphoprotein 1	Downregulated
AA682637	Carbohydrate sulfotransferase 2	Downregulated
AI371874	Toll-like receptor 4 precursor	Upregulated

Table 7: Genes with Differences in the Expression Levels in each subtype of IBD Disorder

GenBank	Description	Expression in CD patients	Expression in UC patients
AA083407	Tripartite motif-containing 22	No change	Downregulated
AA476221	Unnamed protein product	Downregulated	No change
AA495985	Small inducible cytokine A18 precursor (CCL18)	Downregulated	Upregulated
AI123732	EBV-induced G protein-coupled receptor 2 (EBI2)	Downregulated	No change
AA281497	Interferon-gamma receptor alpha 1	Downregulated	No change
R47893	Small inducible cytokine A3 precursor (CCL3)	Downregulated	Upregulated
AA454646	Lymphotoxin-beta receptor	No change	Upregulated
AI298976	Lymphotactin precursor (XCL1)	Downregulated	No change

APPENDIX B: FIGURES

Figure 1: Specificity of IS900-derived FITC-labeled DNA Probe.

The specificity of the DNA probe was evaluated against culture smears from *E. coli* (A), *Staphylococcus aurous* (B), *Mycobacterium. smegmatis* (C), *Mycobacterium avium* subspecies *avium* (D) and MAP (E). The presence of MAP was detected as a yellow color indicating the colocalization of the green FITC-labeled IS900 probe specific for MAP DNA hybridized with corresponding genomic MAP DNA present in the bacterial samples using CSLM. Slides containing non-MAP bacterial culture stained with the propidium iodide (red color) indicating negative colocalization with the fluorescent IS900 probe.

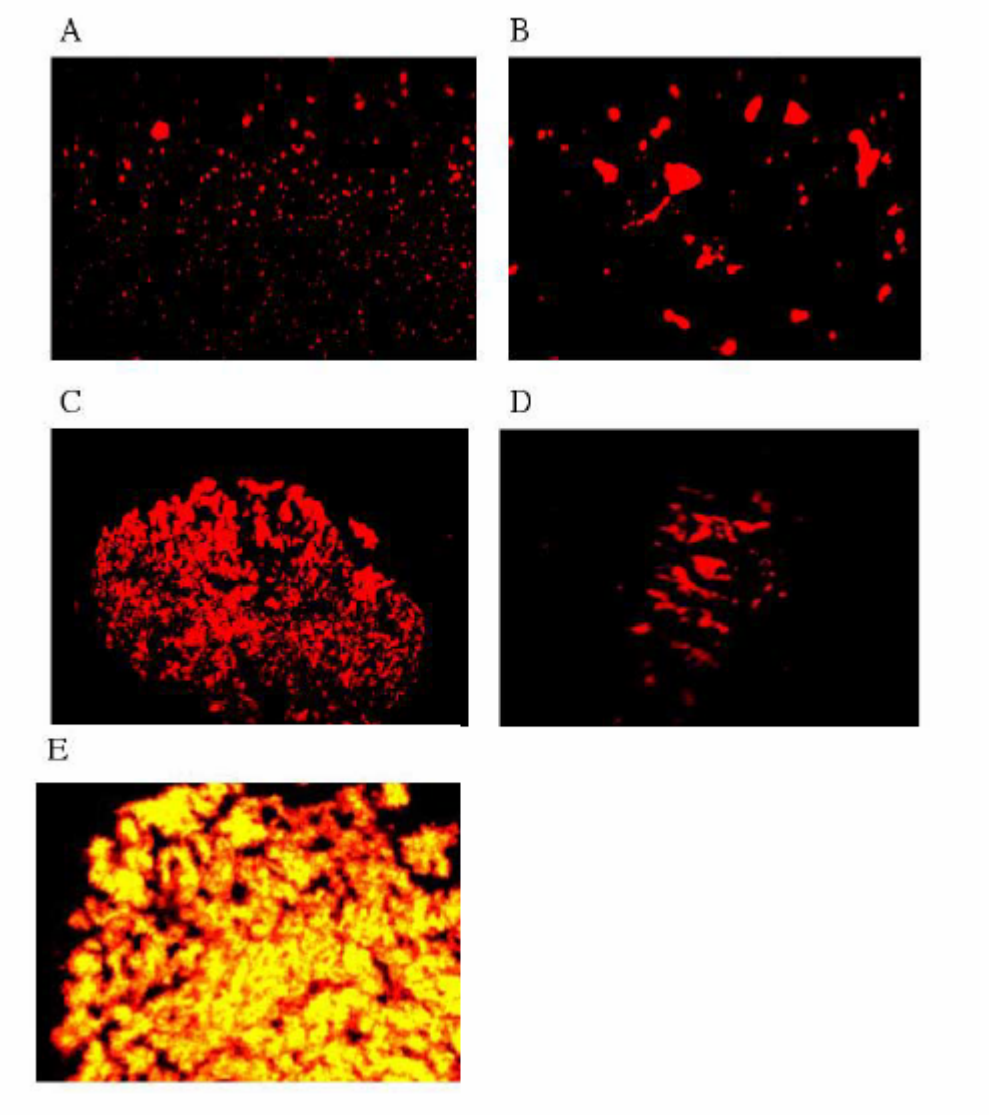
A
B
C
D
E

Figure 2: Detection of MAP in spiked tissue by *in-situ* hybridization.

The optimized *in-situ* hybridization technique was evaluated following the analysis of slides with normal tissue sections from a colon cancer patient (A) and slides with same tissue spiked with MAP culture (B) as visualized by CSLM. The presence of MAP was detected as a yellow color indicating the colocalization of the green FITC-labeled IS900 probe with MAP DNA if present. The red staining observed corresponds to tissue stained with the propidium iodide.

.

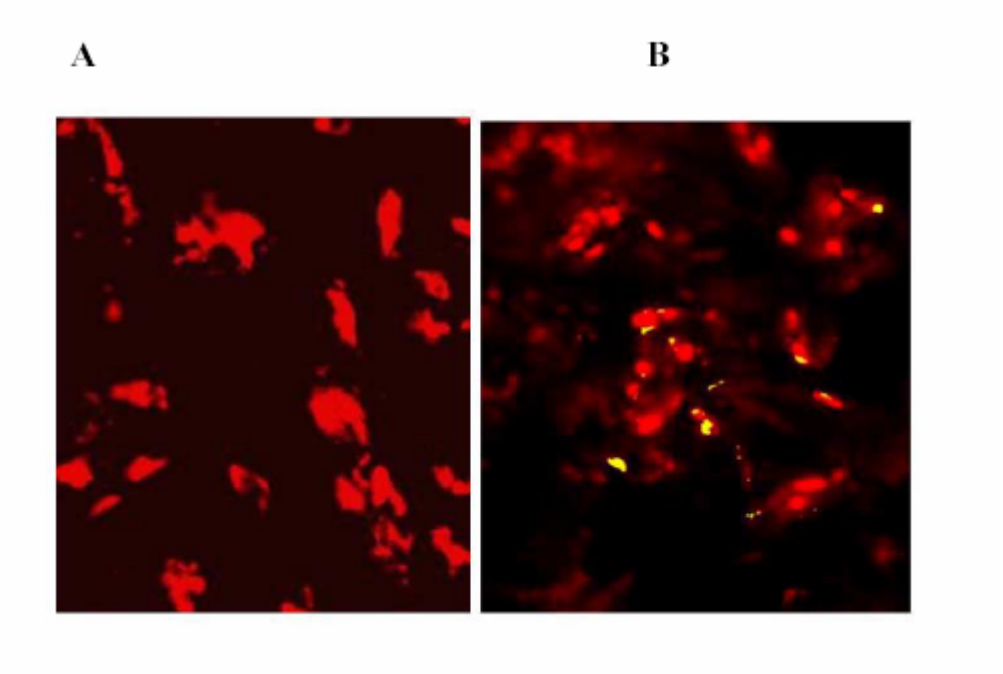
A
B

Figure 3: *In-situ* identification of MAP DNA in CD tissue samples.

CLSM images illustrate the presence or absence of MAP in tissue from three CD patients (A, B and C). I corresponds to inflamed tissue and N corresponds to non-inflamed tissue. The presence of MAP was detected as a yellow color indicating the colocalization of the green FITC-labeled IS900 probe with MAP DNA if present using CSLM. The red staining observed corresponds to tissue stained with the propidium iodide.

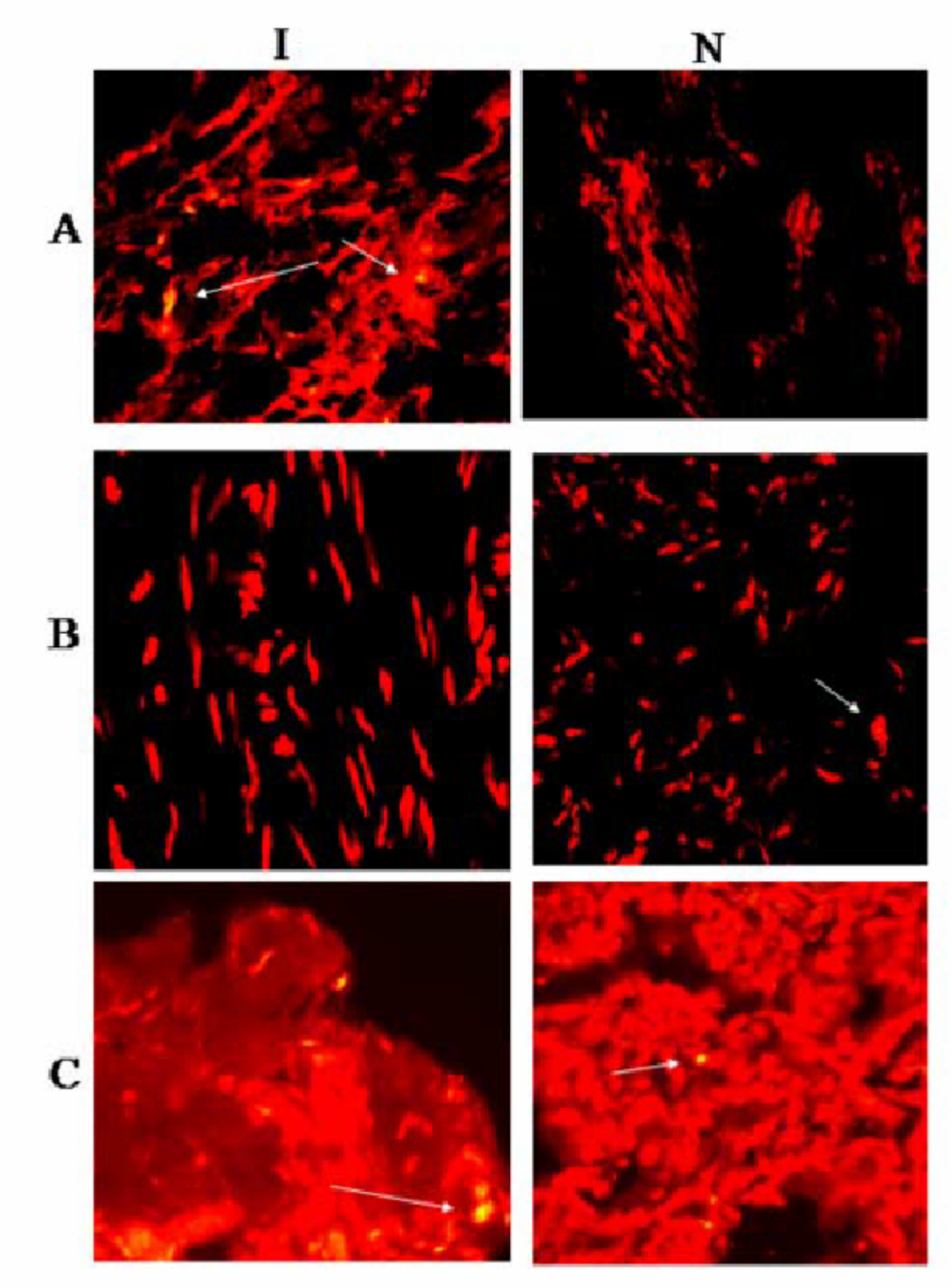
I
N
A
B
C

Figure 4: *In-situ* identification of MAP DNA in non-IBD tissue samples.

CLSM Images illustrate the absence of MAP DNA in tissue from all six non-IBD patients (A-F). MAP DNA, if present, will be visualized as a yellow color indicating the colocalization of the green FITC-labeled IS900 probe with MAP genome using CSLM. The red staining observed corresponds to tissue stained with the propidium iodide.

.

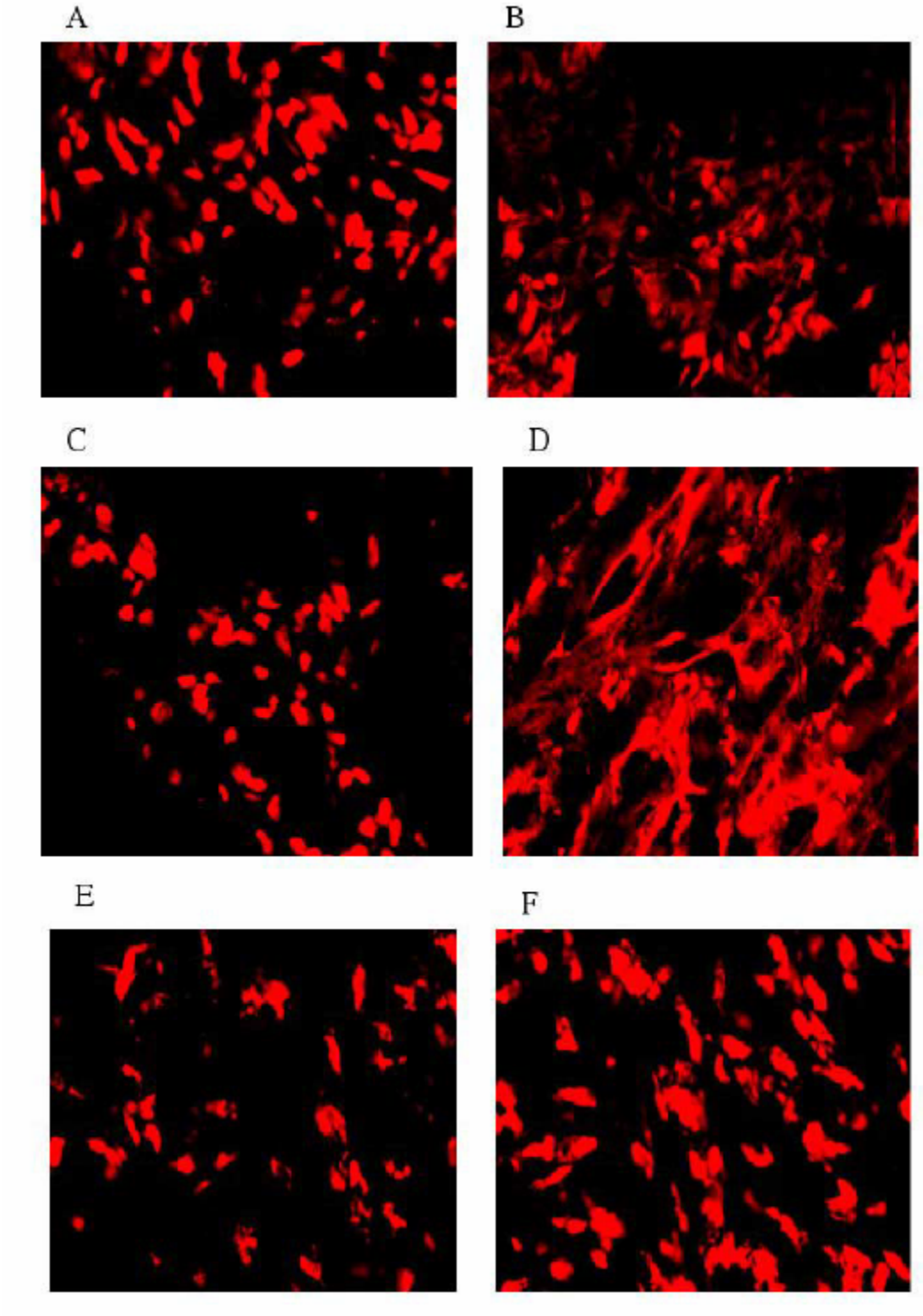
A
B
C
D
E
F

Figure 5: PCR Detection of MAP DNA in Surgical Tissue Samples.

PCR product from the second round of the nested PCR was analyzed on 2% agarose gel. An amplified 298 bp fragment indicates positive sample for MAP DNA. CD: represent tissue samples from CD patients whereas non-IBD represents tissue from colon cancer patients.. NC: negative control, PC: positive control, MK: molecular weight marker. Lanes with odd numbers represent DNA from Inflamed tissue and even numbers represent those from non-inflamed tissue.

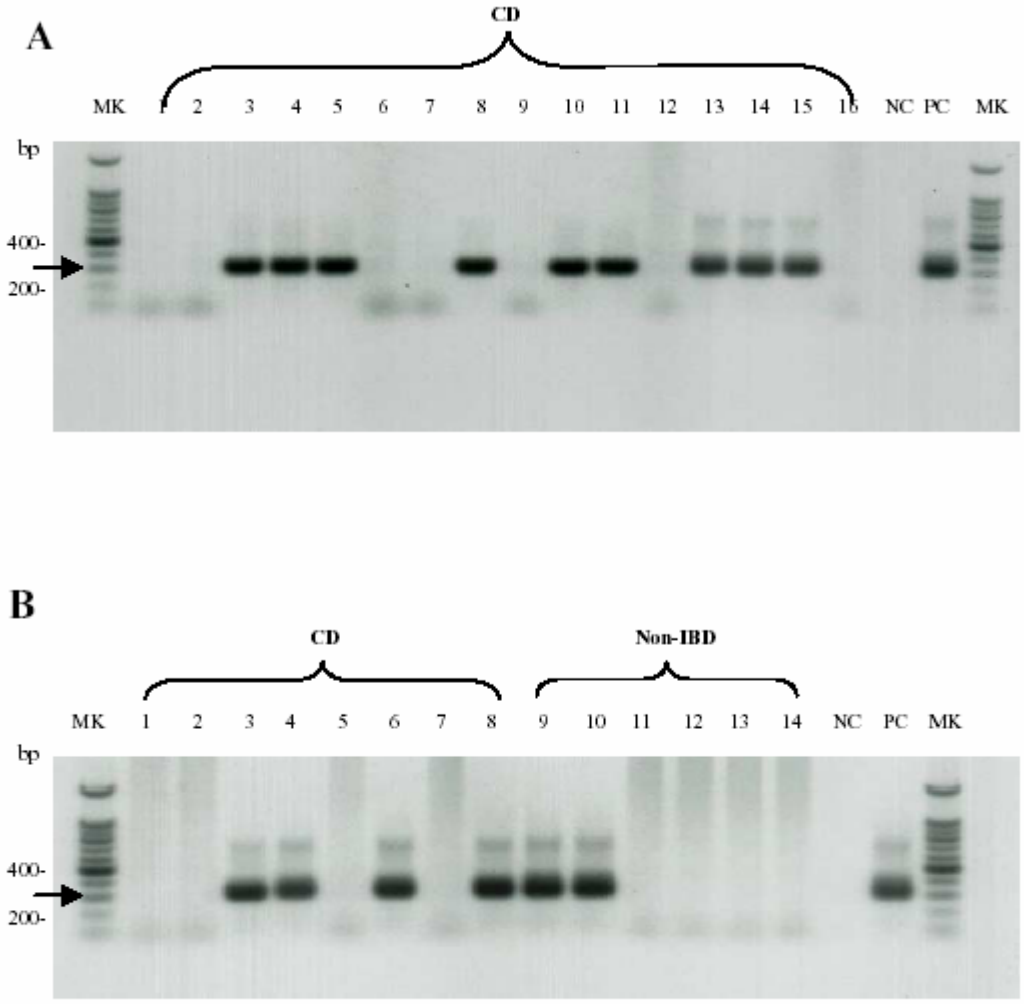
A
CD
MK 1 2 3 4 5 6 7 8 9 10 11 12 13 14 15 16 NC PC MK
bp
400-
200-
B
CD
Non-IBD
MK 1 2 3 4 5 6 7 8 9 10 11 12 13 14 NC PC MK
bp
400-
200-

Figure 6: Nested PCR detection of IS900 DNA Unique to *Mycobacterium avium* subsp *paratuberculosis* (MAP) in Surgical Tissue.

Forty three DNA extracts isolated from homogenized tissue specimens from 17 CD and 2 UC patients were analyzed by nested PCR. Detection of MAP DNA is indicated by the amplification of a 298 bp fragment. Gel A lanes 2, 4, 7, 9, 11, 13, 16, 18, 20, 22, 24 and gel B lanes 4, 7, 10, 13 represent DNA from non-inflamed tissue from 15 CD patients. Gel A lanes 1, 3, 6, 8, 10, 12, 15, 17, 19, 21, 23, 25 and gel B lanes 1, 3, 6, 9, 11 represent DNA from inflamed tissue from 17 CD patients. DNA from lymph nodes tissue from 7 CD patients is shown in gel A lanes 5, 14, 26 and gel B lanes 2, 5, 8, 12. DNA from non-inflamed tissue (lane B16), two inflamed tissue (lanes B17 and B14) and one lymph node tissue (lane B15) from two ulcerative colitis patients is also shown.

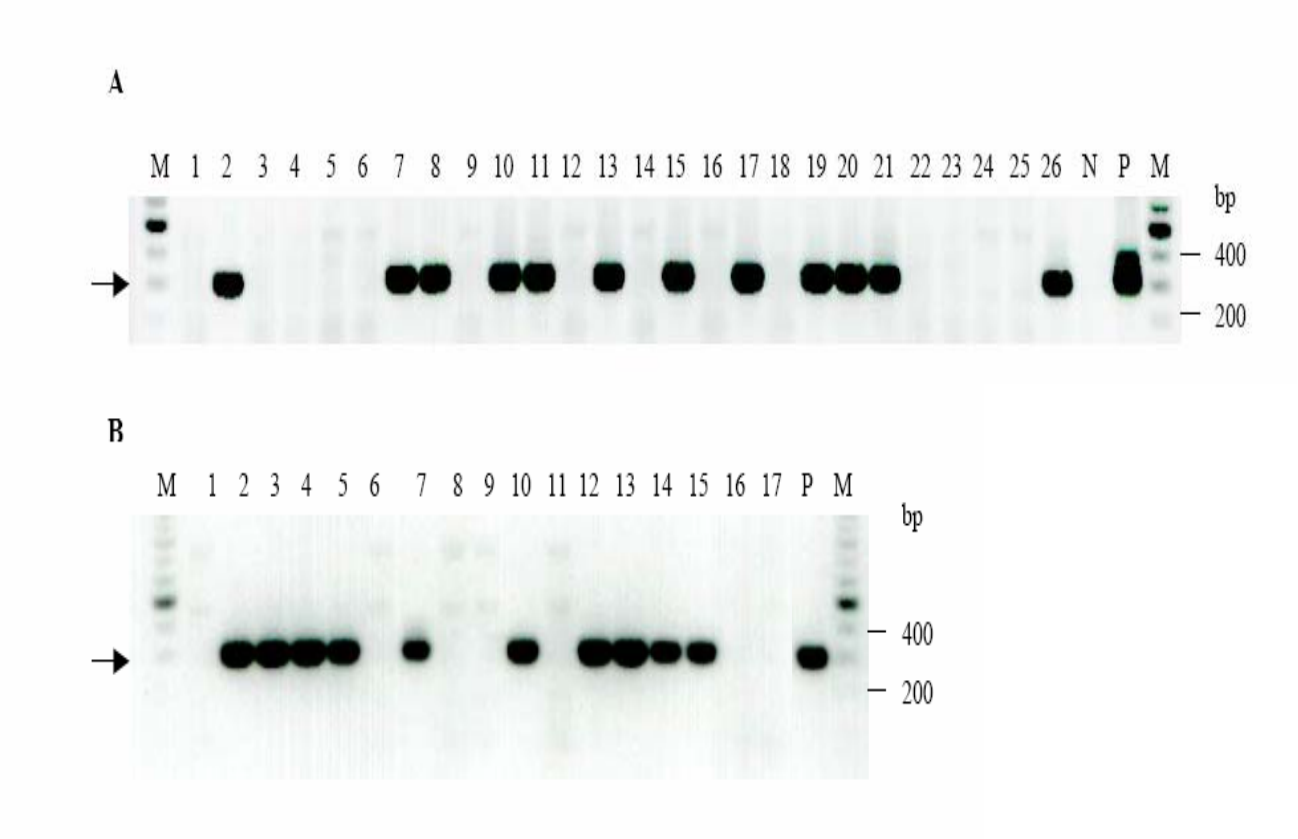
A
M 1 2 3 4 5 6 7 8 9 10 11 12 13 14 15 16 17 18 19 20 21 22 23 24 25 26 N P M
bp
400
200
B
M 1 2 3 4 5 6 7 8 9 10 11 12 13 14 15 16 17 P M
bp
400
200

Figure 7: Confocal Scanning Laser Microscopy (CSLM) Evaluation of the Phagocytosis of FITC-labeled viable and dead bacterial cells by PMN from Healthy subjects.

Following two h exposure of PMN to 10^7 CFU of FITC-labeled viable and dead *Escherichia coli* (A and B), FITC-labeled viable and dead *Mycobacterium tuberculosis* (C and D), and FITC-labeled viable and dead MAP (E and F), the amount of phagocytosed bacteria was detected by green fluorescence. Using the Zeiss image analysis software, a treshold was applied to eliminate pixels with no fluorescence (black) and residual noise from the detector. The only fluorescence detected was the one coming from the inside of the phagocytic cells that is directly proportional to the amount of bacterial cells phagocytosed. Viable and dead bacterial cells were localized scattered throughout the cytoplasm inside healthy PMN indicating the disintegration of these bacteria inside the macrophages.

.

A

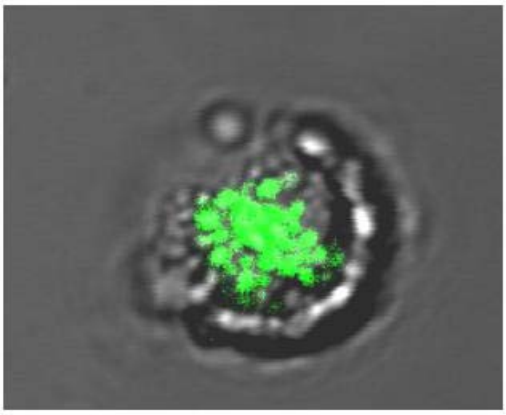

B

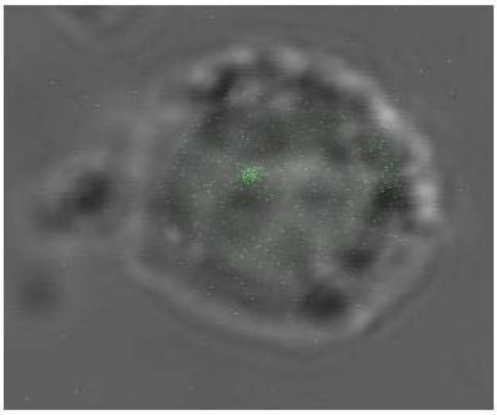

C

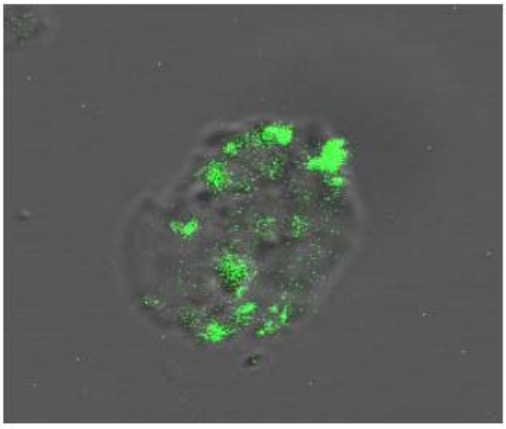

D

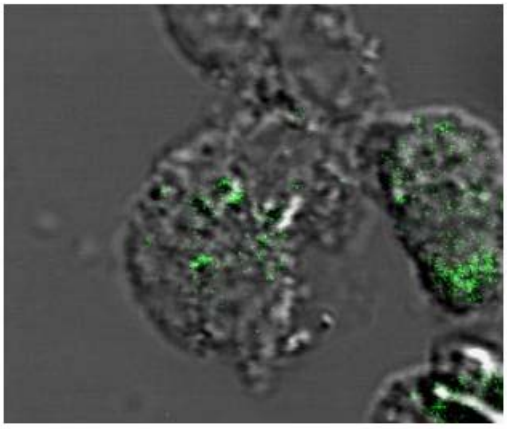

E

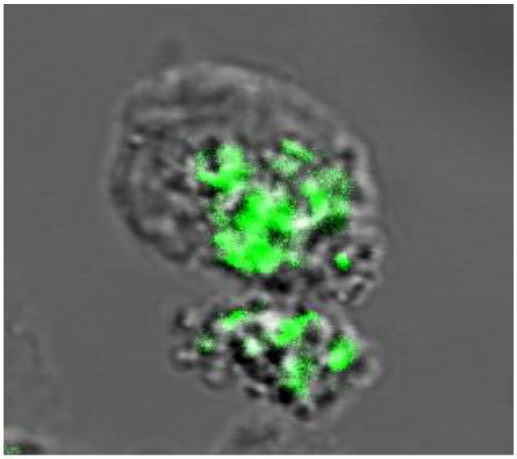

F

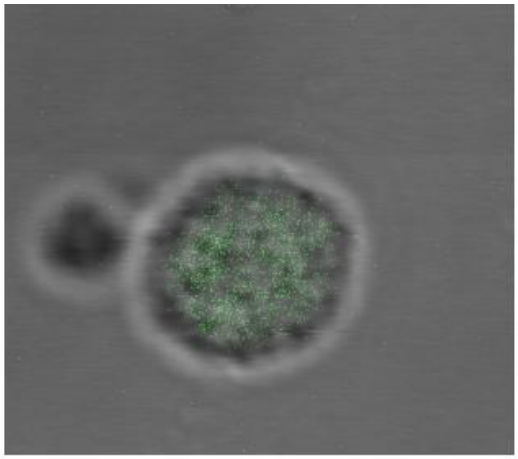

Figure 8: Confocal Scanning Laser Microscopy (CSLM) Evaluation of the Phagocytosis of FITC-labeled viable and dead bacterial cells by PMN from UC subjects.

Following two h exposure of PMN to 10^7 CFU of FITC-labeled viable and dead *Escherichia coli* (A and B), FITC-labeled viable and dead *Mycobacterium tuberculosis* (C and D), and FITC-labeled viable and dead MAP (E and F), the amount of phagocytosed bacteria was detected by green fluorescence. Using the Zeiss image analysis software, a treshold was applied to eliminate pixels with no fluorescence (black) and residual noise from the detector. The only fluorescence detected was the one coming from the inside of the phagocytic cells that is directly proportional to the amount of bacterial cells phagocytosed. Viable and dead bacterial cells were localized scattered throughout the cytoplasm inside healthy PMN indicating the disintegration of these bacteria inside the macrophages.

.

A

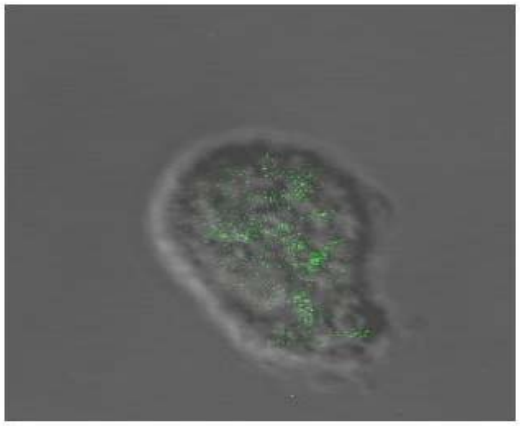

B

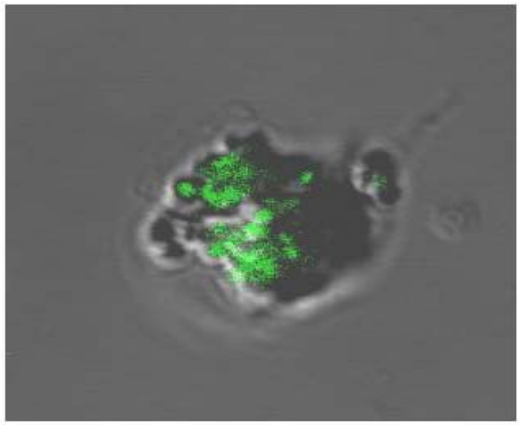

C

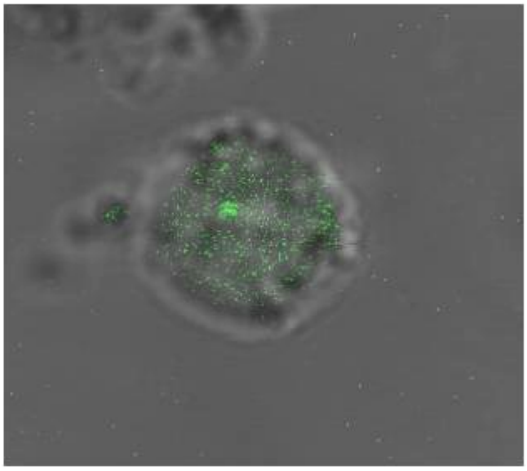

D

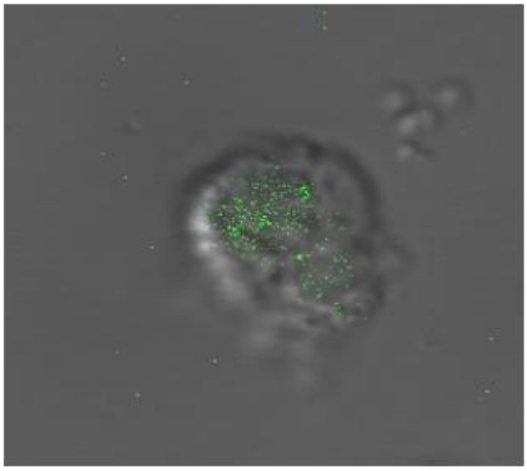

E

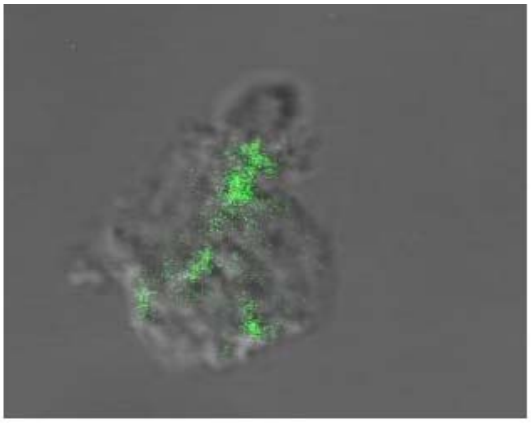

F

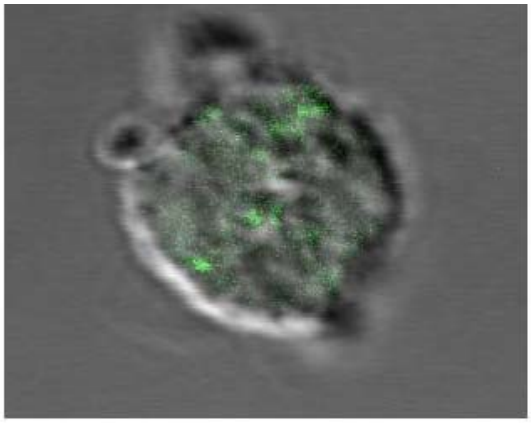

Figure 9: Confocal Scanning Laser Microscopy (CSLM) Evaluation of the Phagocytosis of FITC-labeled viable and dead bacterial cells by PMN from CD subjects.

Following two h exposure of PMN to 10^7 CFU of FITC-labeled viable and dead *Escherichia coli* (A and B), FITC-labeled, dead *Mycobacterium tuberculosis* (D), and FITC-labeled viable and dead MAP (E and F), the amount of phagocytosed bacteria was detected by green fluorescence. Using the Zeiss image analysis software, a treshold was applied to eliminate pixels with no fluorescence (black) and residual noise from the detector. The only fluorescence detected was the one coming from the inside of the phagocytic cells that is directly proportional to the amount of bacterial cells phagocytosed. Viable MAP (E) was concentrated in phagosomes closer to the cytoplasmic membrane compared to the dead MAP and other bacterial cells seen scattered throughout the cytoplasm. Viable MAP behaved in a way similarly to viable M. tuberculosis where a visible phagocytic vacuole containing bacteria is formed from the membrane (C).

A

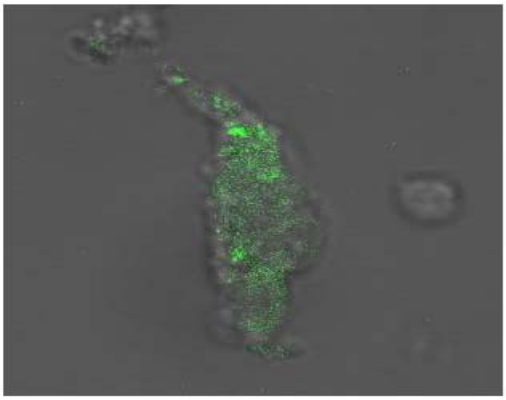

B

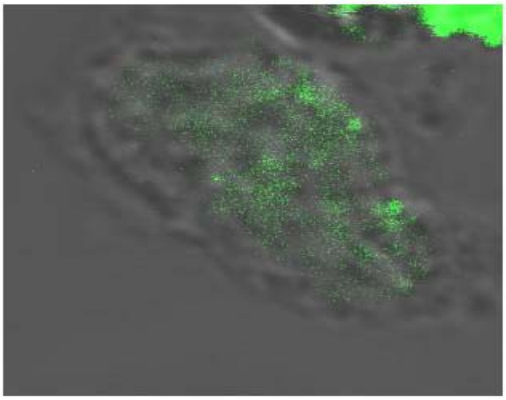

C

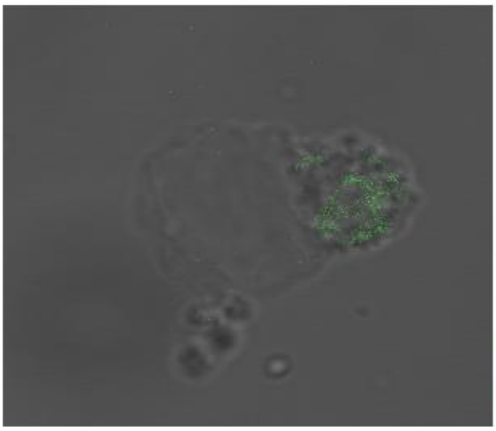

D

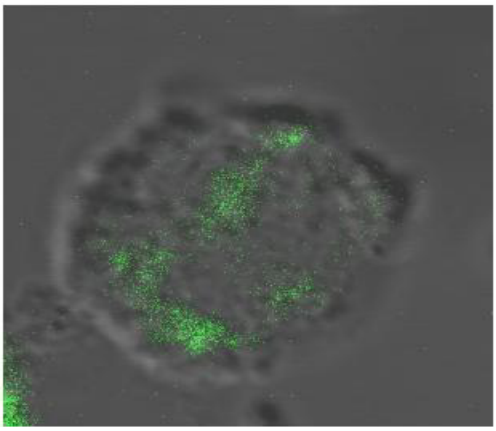

E

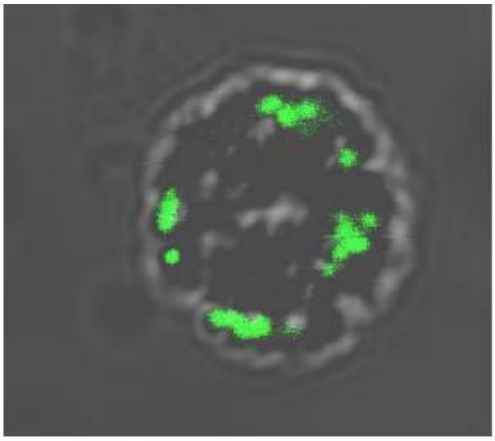

F

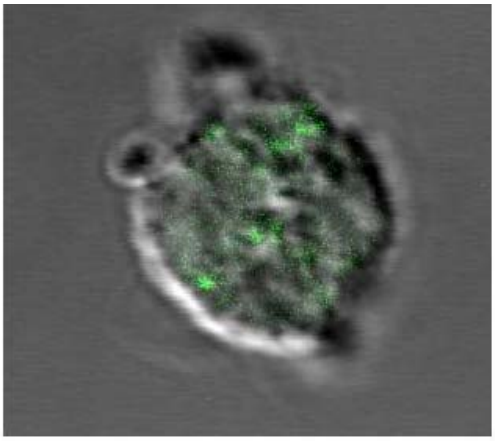

Figure 10: Confocal Scanning Laser Microscopy (CSLM) of culture PMN from CD subjects infected with viable bacteria.

Following two h exposure of PMN to 10^7 CFU of FITC-labeled viable *Escherichia coli* (A), FITC-labeled viable *Mycobacterium tuberculosis* (B), and FITC-labeled viable MAP (C). The amount of phagocytosed bacteria was detected by green fluorescence. Using the Zeiss image analysis software, a treshold was applied to eliminate pixels with no fluorescence (black) and residual noise from the detector. The only fluorescence detected was the one coming from the inside of the phagocytic cells that is directly proportional to the amount of bacterial cells phagocytosed. Viable MAP (C) was concentrated in phagosomes closer to the cytoplasmic membrane as well as viable TB (B).

A

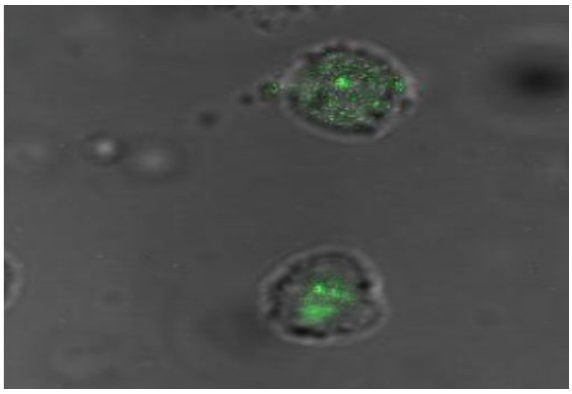

B

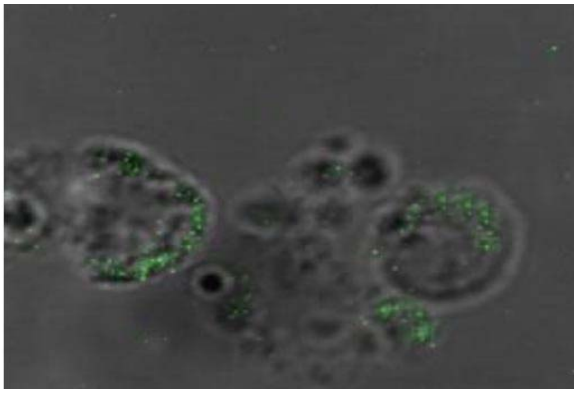

C

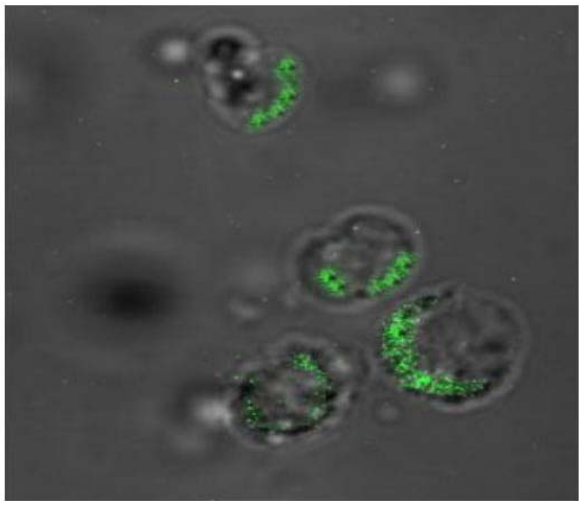

Figure 11: Biological themes predicted by MeV with EASE microarray analysis software.

We found that 17% (5630 genes) of the total number of genes was differentially expressed in both IBD disorders compared to the reference pooled sample. These genes were distributed mainly within four biological themes classified as cellular processes (38%), physiological processes (26%), intracellular genes (18%), and genes involved in metabolism (18%).

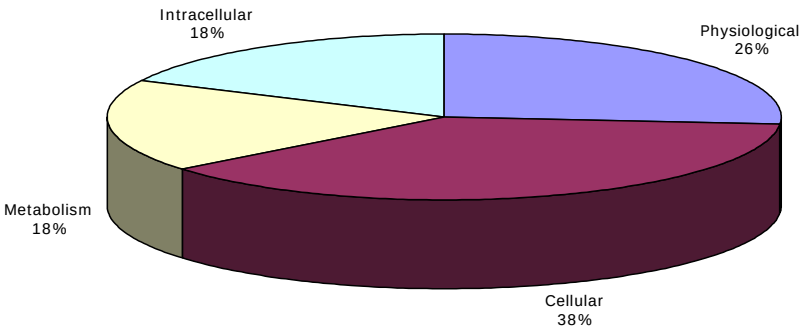
Intracellular
18%
Physiological
26%
Metabolism
18%
Cellular
38%

Figure 12: Overall variation in the immune response gene expression patterns in human white blood cells.

Of the 5630 genes differentially expressed in the experimental samples, 238 genes belonged to genes involved in the immune response. Eight clusters are shown and the differentially expressed genes are boxed either in red boxes (genes that were unique for each IBD disorder) or blue boxes (common genes present in both IBD disorders). The expression levels of the IFNGR1 gene is also indicated by a plus sign next to the red box. Each element is red, green, black, or gray. Black elements have a log ratio (Cy5/Cy3) of 0, while green elements have a log ratio of less than 0 and red elements have a log ratio greater than 0. The further the ratio from 0, the brighter the element is. Gray elements have invalid values and are not used in any analysis.

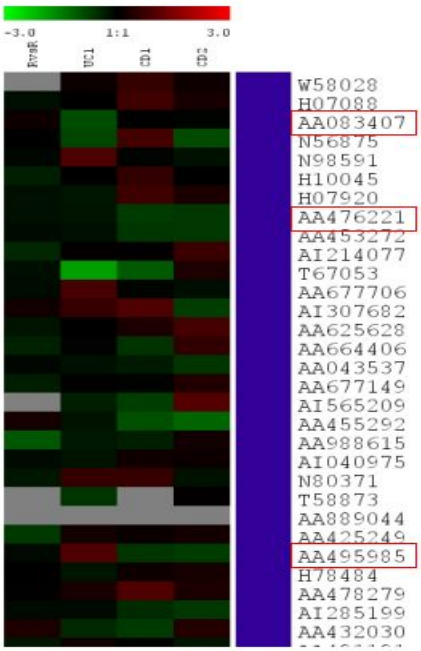
-3.0
1:1
3.0
RvsR
UC1
CD1
CD2
W58028
H07088
AA083407
N56875
N98591
H10045
H07920
AA476221
AA453272
AI214077
T67053
AA677706
AI307682
AA625628
AA664406
AA043537
AA677149
AI565209
AA455292
AA988615
AI040975
N80371
T58873
AA889044
AA425249
AA495985
H78484
AA478279
AI285199
AA432030

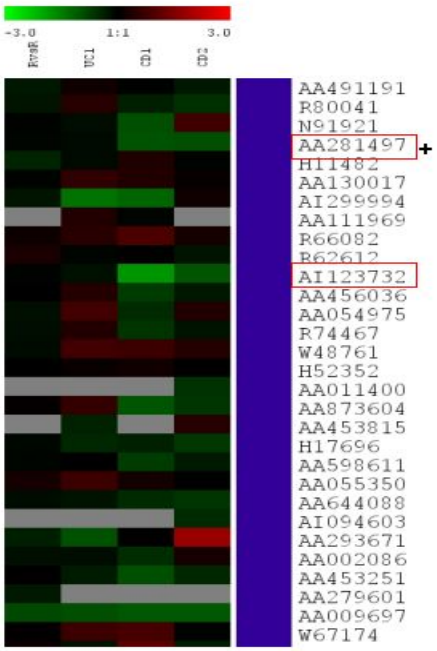
-3.0
1:1
3.0
RvsR
UC1
CD1
CD2
AA491191
R80041
N91921
AA281497
H11482
AA130017
AI299994
AA111969
R66082
R62612
AI123732
AA456036
AA054975
R74467
W48761
H52352
AA011400
AA873604
AA453815
H17696
AA598611
AA055350
AA644088
AI094603
AA293671
AA002086
AA453251
AA279601
AA009697
W67174

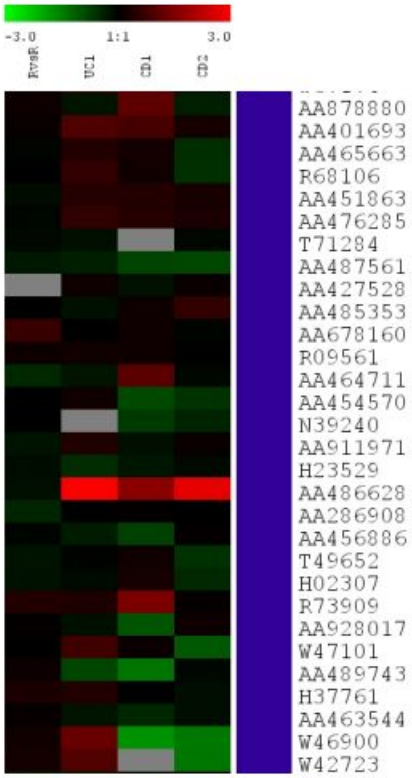
-3.0
1:1
3.0
RvsR
UC1
CD1
CD2
AA878880
AA401693
AA465663
R68106
AA451863
AA476285
T71284
AA487561
AA427528
AA485353
AA678160
R09561
AA464711
AA454570
N39240
AA911971
H23529
AA486628
AA286908
AA456886
T49652
H02307
R73909
AA928017
W47101
AA489743
H37761
AA463544
W46900
W42723

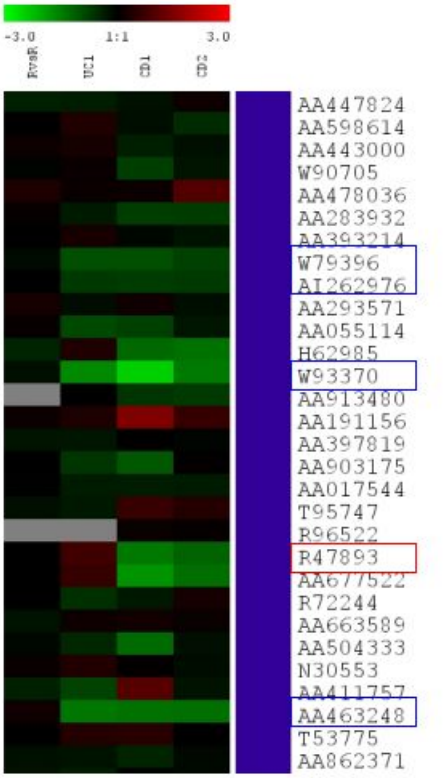
-3.0
1:1
3.0
RvsR
UC1
CD1
CD2
AA447824
AA598614
AA443000
W90705
AA478036
AA283932
AA393214
W79396
AI262976
AA293571
AA055114
H62985
W93370
AA913480
AA191156
AA397819
AA903175
AA017544
T95747
R96522
R47893
AA677522
R72244
AA663589
AA504333
N30553
AA411757
AA463248
T53775
AA862371

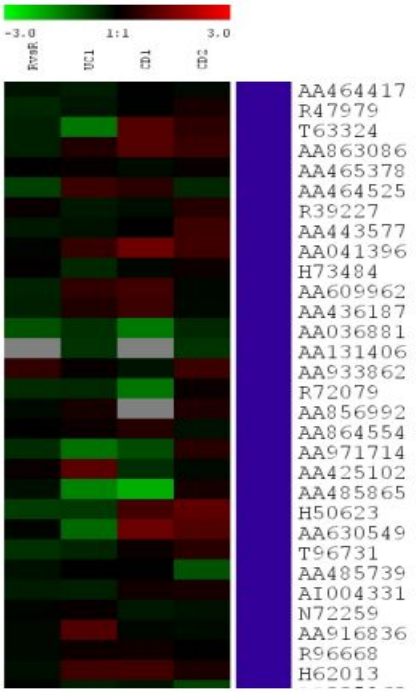
-3.0
1:1
3.0
AA464417
R47979
T63324
AA863086
AA465378
AA464525
R39227
AA443577
AA041396
H73484
AA609962
AA436187
AA036881
AA131406
AA933862
R72079
AA856992
AA864554
AA971714
AA425102
AA485865
H50623
AA630549
T96731
AA485739
AI004331
N72259
AA916836
R96668
H62013

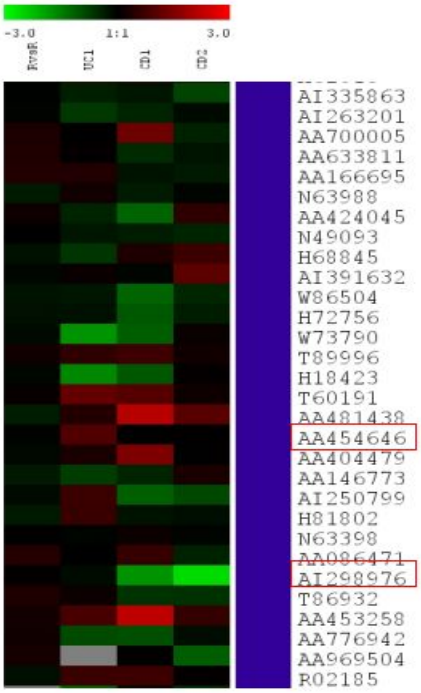
-3.0
1:1
3.0
AI335863
AI263201
AA700005
AA633811
AA166695
N63988
AA424045
N49093
H68845
AI391632
W86504
H72756
W73790
T89996
H18423
T60191
AA481438
AA454646
AA404479
AA146773
AI250799
H81802
N63398
AA086471
AI298976
T86932
AA453258
AA776942
AA969504
R02185

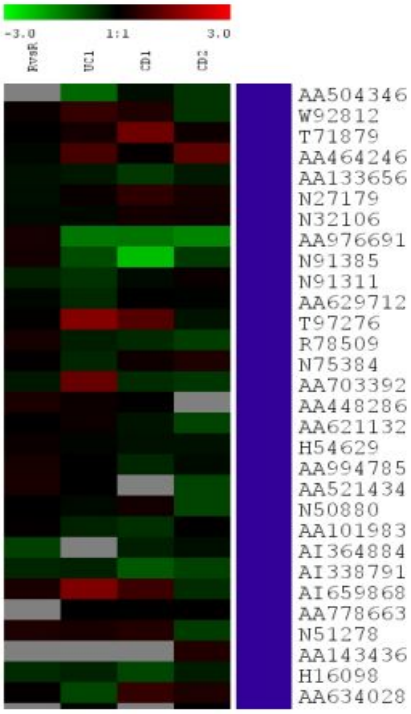
-3.0
1:1
3.0
AA504346
W92812
T71879
AA464246
AA133656
N27179
N32106
AA976691
N91385
N91311
AA629712
T97276
R78509
N75384
AA703392
AA448286
AA621132
H54629
AA994785
AA521434
N50880
AA101983
AI364884
AI338791
AI659868
AA778663
N51278
AA143436
H16098
AA634028

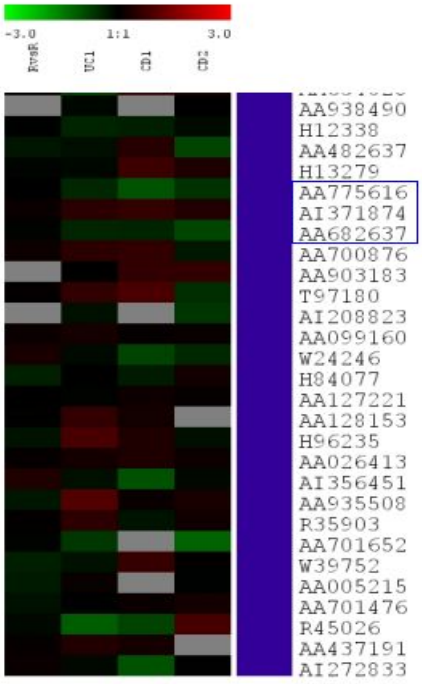
-3.0
1:1
3.0
AA938490
H12338
AA482637
H13279
AA775616
AI371874
AA682637
AA700876
AA903183
T97180
AI208823
AA099160
W24246
H84077
AA127221
AA128153
H96235
AA026413
AI356451
AA935508
R35903
AA701652
W39752
AA005215
AA701476
R45026
AA437191
AI272833

LIST OF REFERENCES

1. Anumanthan A, Bensussan A, Boumsell L, et al. Cloning of BY55, a novel Ig superfamily member expressed on NK cells, CTL, and intestinal intraepithelial lymphocytes. *J Immunol* 1998; 161(6): 2780-90.
2. Becker KG**,** Nagle JW**,** Canning RD, et al. Rapid isolation and characterization of 118 novel C2H2-type zinc finger cDNAs expressed in human brain. *Hum Mol Genet* 1995; 4 (4): 685-91.
3. Biggerstaff J, Amirkhosravi A, Francis JL. Three Dimensional Quantitation of Tumor Microvessel Density by Confocal Laser Scanning Microscopy. Cell Vision. *J Anal Morph* 1998; 4 (2): 152-3.
4. Birkenbach M, Josefsen K, Yalamanchili R, et al. Epstein-Barr virus-induced genes: first lymphocyte-specific G protein-coupled peptide receptors. *J Virol* 1993; 67(4): 2209-20.
5. Bouma G, Strober W. The immunological and genetic basis of inflammatory bowel disease. *Nature Reviews Immunology* 2003; 3: 521-533.
6. Britton WJ, Lockwood DN. Leprosy. *Lancet* 2004; 363(9416): 1209-19.
7. Bull TJ, McMinn EJ, Sidi-Boumedine K, et al. Detection and verification of *Mycobacterium avium* subsp *paratuberculosis* in fresh ileocolonic mucosal biopsy specimens from individuals with and without Crohn's disease. *J Clin Microbiol* 2003; 41: 2915–23.

8. Camoglio L, Te Velde AA, Tigges AJ, et al. Altered expression of interferon-gamma and interleukin-4 in inflammatory bowel disease. *Inflamm Bowel Dis* 1998; 4: 285-90.
9. Chen G, Saibil F, Morava-Protzner I. Two for one: Coexisting ulcerative colitis and Crohn's disease. *Can J Gastroenterol* 2002; 16: 29–34.
10. Chiodini RJ, Van Kruiningen HJ, Merkal RS, et al. Characteristics of an Unclassified Mycobacterium species Isolated from Patients with Crohn's Disease. *J. Clin. Microbiol* 1984; 20: 966-971.
11. Chiodini RJ, Van Kruiningen HJ, Thayer WR, et al. Spheroplastic phase of mycobacteria isolated from patients with Crohn's disease. *J Clin Microbiol* 1986; 27: 357-63.
12. Chiodini RJ. Crohn's disease and the mycobacterioses: a review and comparison of two diseases entities. *Clin Microbiol Rev* 1989; 2: 90-117.
13. Cocchi F, DeVico AL, Garzino-Demo A, et al. Identification of RANTES, MIP-1 alpha, and MIP-1 beta as the major HIV-suppressive factors produced by CD8+ T cells. *Science* 1995; 270(5243): 1811-5.
14. Collins MT, Lisby G, Moser C, et al. Results of Multiple Diagnostic Tests for *Mycobacterium avium* subsp. *paratuberculosis* in Patients with Inflammatory Bowel Disease and in Controls. *J. Clin. Microbiol.* 2000; 38: 4373-81.
15. Cooper AM, Dalton DK, Stewart TA, et al. Disseminated Tuberculosis in Interferon-gamma Gene-disrupted Mice. *J Exp Med* 1993; 178: 2243-47.
16. Crohn B, Ginzburg K, Oppenheimer GD. Regional Ileitis: a Pathological and Clinical Entity. *J. Am. Med. Assoc.* 1932; 99: 1323-1329.
17. Dalziel TK. Chronic Interstitial Enteritis. *Br. Med. J.* 1913; 2: 1068-1070.

18. Dell'Isola B, Poyart C, Goulet O, et al. Detection of *Mycobacterium paratuberculosis* by Polymerase Chain Reaction in Children with Crohn's Disease. *J. Infect. Dis* 1994; 169: 449-451.

19. Dieckgraefe BK, Korzenik JR. Treatment of active Crohn's disease with recombinant human granulocyte-macrophage colony-stimulating factor. *Lancet.* 2002; 360(9344): 1478-80.

20. Dorman SE, Holland SM. Mutation in the signal -transducing chain of the interferon - - receptor and susceptibility to mycobacterial infection. *J Clin Invest.* 1998; 101: 2364-9.

21. Drumm B, Vaughan D. Granulocyte-macrophage colony-stimulating factor for Crohn's disease. *Lancet.* 2003; 361(9371): 1830.

22. Ebert EC, Bhatt BD, Liu S, et al. Induction of Suppressor Cells by *Mycobacterium paratuberculosis* Antigen in Inflammatory Bowel Disease. *Clin. Exp. Immunol.* 1991; 83: 320-325.

23. El-Zaatari FAK, Naser SA, Engstrand L, et al. Identification and Characterization of *Mycobacterium paratuberculosis* Recombinant Proteins Expressed in *E. coli. Cur. Microbiol.* 1994; 29: 177-184.

24. El-Zaatari FAK, Naser SA, Hulten K, et al. Characterization of *Mycobacterium paratuberculosis* p36 antigen and its seroreactivities in Crohn's Disease. *Curr Microbiol*. 1999; 39: 115-119.

25. El-Zaatari FAK, Naser SA, Engstrand L, et al. Nucleotide Sequence Analysis and Seroreactivities of the 65K Heat Shock Protein from *Mycobacterium paratuberculosis*. *Clin. Diag. Lab. Immunol.* 1995; 2: 657-664.

26. El-Zaatari FAK, Naser SA, Graham DY. Characterization and seroreactivity of a specific *Mycobacterium paratuberculosis* recombinant clone expressing 35K antigen with clinical and subclinical johne's disease. *J Clin Microbiol.* 1997; 35: 1794-1799.

27. Everhart JE. Digestive diseases in the United States: Epidemiology and impact; *NIH Publication* 1994; 94: 1447.

28. Geijtenbeek TBH, Van Vliet SJ, Koppel EA, et al. Mycobacteria target DC-SIGN to suppress dendritic cell function. *J. Exp. Med* 2003; 197: 7-17.

29. Girardin SE, Boneca IG, Viala J, et al. Peptidoglycan molecular requirements allowing detection by Nod1 and Nod2. *J. Biol. Chem.* 2003; 278: 8869-8872.

30. Glasser AL, Boudeau J, Barnich N, et al. Adherent Invasive *Escherichia coli* Strains from Patients with Crohn's Disease Survive and Replicate within Macrophages without Inducing Host Cell Death. *Infect Immun.* 2001; 69 (9): 5529–5537.

31. Glienke J, Sobanov Y, Brostjan C, et al. The genomic organization of NKG2C, E, F, and D receptor genes in the human natural killer gene complex. *Immunogenetics* 1998; 48 (3): 163-73.

32. Grant IR, Ball HJ, Rowe MT. Incidence of *Mycobacterium paratuberculosis* in bulk raw and commercially pasteurized cows' milk from approved dairy processing establishments in the United Kingdom. *Appl Environ Microbiol* 2002; 68: 2428–35.

33. Green EP, Tizard ML, Moss MT, et al. Sequence and characteristics of IS900, an insertion element identified in a human Crohn's disease isolate of *Mycobacterium paratuberculosis*. *Nuc Aci Res* 1989; 17:9063–73.

34. Greenstein RJ, Greenstein AJ. Is There Clinical, Epidemiological, and Molecular Evidence for Two Forms of Crohn's Disease? *Mol. Med. Today.* 1995; 1(7): 343-348.

35. Greenstein AJ, Lachman P, Sachar DB, et al. Perforating and Non-perforating Indications for Repeated Operations in Crohn's Disease: Evidence for Two Clinical Forms. *Gut.* 1988; 29: 588-592.

36. Gwozdz JM, Thompson KG, Murray A, et al. Use of polymerase chain reaction assay for the detection of *Mycobacterium avium* subspecies *paratuberculosis* in blood and liver biopsies from experimentally infected sheep. *Aust Vet J* 2000; 78: 622–4.

37. Harvey RF, Bradshaw JM. A simple index of Crohn's-disease activity. *Lancet* 1980; 1: 514.

38. Hedge P, Qi R, Abernathy R, et al. A concise guide to cDNA microarray analysis. Biotechniques 2000; 29: 548-562.

39. Hendrickson BA, Gokhale R, Cho JH. Clinical Aspects and Pathophysiology of Inflammatory Bowel Disease. *Clin Microbiol Rev* 2002; 15(1): 79-94.

40. Hermon-Taylor J, Barnes N, Clarke C, et al. *Mycobacterium paratuberculosis* Cervical Lymphadenitis Followed Five Years Later by Terminal Ilieitis Similar to Crohn's Disease. *Br. Med. J.* 1998; 316:449-453.

41. Hieshima K, Imai T, Baba M, et al. *J Immunol* 1997; 159 (3): 1140-9.

42. Hornef MW, Wick MJ, Rhen M, et al. Bacterial strategies for overcoming host innate and adaptive immune responses. *Nat Immunol.* 2002; 3(11): 1033-40.

43. Hugot JP, Chamaillard M, Zouali H, et al. Association of NOD2 leucine-rich repeat variants with susceptibility to Crohn's disease. *Nature* 2001; 411: 599–603.

44. Jouanguy E, Altare F, Lamhamedi S, et al. Interferon-gamma receptor Deficiency in an Infant with Fatal Bacille Calmette-Guerin Infection. *N Engl J Med.* 1996; 335: 1956-61.

45. Jouanguy E, Lamhamedi S, Lammas D, et al. A human IFNGR1 small deletion hotspot associated with dominant susceptibility to mycobacterial infection. *Nat Genet* 1999; 21: 370-78.

46. Jouanguy E, Lamhamedi-Cherridi S, Altare F, et al. Partial interferon - - receptor 1 deficiency in a child with tuberculoid bacillus Calmetter-Guerin infection and a sibling with clinical tuberculosis. *J Clin Invest.* 1997; 100: 2658-64.

47. Kim DS, Jeon YG, Shim TS, et al. The value of interleukin-12 as an activity marker of pulmonary sarcoidosis. *Vasc Diffuse Lung Dis.* 2000; 17: 271-6.

48. Kobayashi K, Blaser MJ, Brown WR. Immunohistochemical examination for mycobacteria in intestinal tissues from patients with Crohn's disease. *Gastroenterol* 1989; 96: 1009-15.

49. Koets ADP, Rutten VP, de Boer M, et al. Differential changes in heat shock protein-, lipoarabinomannan-, and purified protein derivative-specific immunoglobulin G1 and G2 isotype responses during bovine *Mycobacterium avium* subsp. *paratuberculosis* infection. *Infect Immun*. 2001; 69: 1492-1498.

50. Kohri K, Suzuki Y, Yoshida K, et al. Molecular cloning and sequencing of cDNA encoding urinary stone protein, which is identical to osteopontin. *Biochem. Biophys. Res. Commun.* 1992; 184: 859-864.

51. Li X, Tedder TF. CHST1 and CHST2 sulfotransferases expressed by human vascular endothelial cells: cDNA cloning, expression, and chromosomal localization. *Genomics* 1999; 55: 345-347.

52. Lisby G, Andersen J, Engbaek K, et al. *Mycobacterium paratuberculosis* in intestinal tissue from patients with Crohn's disease demonstrated by a nested primer polymerase chain reaction. *Scand J Gastroenterol* 1994; 29: 923–9.

53. Markesich DC, Graham DY, Yoshimura HH. Progress in culture and subculture of spheroplasts and fastidious acid bacilli isolated from intestinal tissues. *J Clin Microbiol* 1988; 26: 1600-03.

54. Markesich DC, Sawai ET, Butel JS, et al. Humoral Immune Response to Stress (Heat Shock) Proteins. *Dig Dig. Dis. Sci.* 1991; 36: 454-460.

55. McFadden JJ, Butcher PD, Chiodini R, et al. Crohn's disease-isolated mycobacteria are identical to M. para, as determined by DNA probes that distinguish between mycobacterial species. *J Clin Microbiol* 1987; 25: 796–801.

56. Medzhitov R, Preston-Hurlburt P, Janeway CA Jr. A human homologue of the Drosophila Toll protein signals activation of adaptive immunity. *Nature* 1997; 388:394-397.

57. Mishina D, Katsel P, Brown ST, et al. On the etiology of Crohn disease. *Proc Natl Acad Sci* U S A. 1996; 93: 9816–20.

58. Mohagheghpour N, van Vollenhoven A, Goodman J, et al. Interaction of *Mycobacterium avium* with human monocyte-derived dendritic cells. *Infect Immun.* 2000; 68: 5824-9.

59. Moss MT, Sanderson JD, Tizard MLV, et al. Polymerase Chain Reaction of *Mycobacterium paratuberculosis* and *Mycobacterium avium* subsp *silvaticum* in Long Term Cultures from Crohn's Disease and Control Tissues. *Gut.* 1992; 33:1209-1213.

60. Mulder CJJ, Tytgat GNJ. Is Crohn's Disease a Mycobacterial Disease?. 1st ed. Dordrecht: Kluwer Academic Publishers; 1992

61. Naser SA, Hulten K, Shafran I, et al. Specific seroreactivity of Crohn's disease patients against p35 and p36 antigens of *M. avium* subsp. *paratuberculosis. Vet Microbiol.* 2000; 77(3-4): 497-504.

62. Naser SA, Schwartz D, Shafran I. Isolation of *Mycobacterium avium* subsp *paratuberculosis* from Breast Milk of Crohn's Disease Patients. *Am J Gastroenterol* 2000; 95(4):1094-1095.

63. Naser SA, Shafran I, Schwartz D, et al. In situ identification of mycobacteria in Crohn's disease patient tissue using confocal scanning laser microscopy. *Mol Cel Probes* 2002; 16: 41–8.

64. Naser SA, Ghobrial G, Romero C, et al. Culture of *Mycobacterium avium* subspecies *paratuberculosis* from the blood of patients with Crohn's disease. *Lancet.* 2004; 364: 1039-44.

65. Naser SA, Shafran I, El-Zaatari FAK. *Mycobacterium avium* subsp. *paratuberculosis* in Crohn's disease is serologically positive. *Clin Diag Lab Immunol.* 1999; 6: 282.

66. Naser SA, Hulten K, Shafran I, et al. Specific seroreactivity of Crohn's disease patients against p35 and p36 antigens of *M. avium* subsp. *paratuberculosis. Vet Microbiol.* 2000; 77: 497-504.

67. Newport MJ, Huxley CM, Huston S, et al. A mutation in the interferon- -receptor gene and susceptibility to mycobacterial infection. *N Engl J Med.* 1996; 335: 1941-9.

68. Ogura Y, Bonen DK, Inohara N, et al. A frame shift mutation in NOD2 associated with susceptibility to Crohn's disease. *Nature* 2001; 411: 603–6.

69. Pallone F, Monteleone G. Interleukin 12 and Th1 responses in inflammatory bowel disease. *Gut.* 1998; 43: 735-6.

70. Rosen SDú. Endothelial ligands for L-selectin: from lymphocyte recirculation to allograft rejection. *Am. J. Pathol.* 1999; 155: 101320.

71. Sanderson JD, Moss MT, Tizard ML, et al. *Mycobacterium paratuberculosis* DNA in Crohn's Disease Tissue. *Gut.* 1992; 33: 890-896.

72. Sands BE. From symptoms to diagnosis: clinical distinctions among various forms of intestinal inflammation. *Gastroenterol* 2004; 126: 1518–32.

73. Sands BE, Anderson FH, Bernstein CN, et al. Infliximab maintenance therapy for fistulizing Crohn's disease. *N Engl J Med.* 2004; 350(9): 876-85.

74. Saxegaard F. Isolation of *Mycobacterium paratuberculosis* from intestinal mucosa and mesenteric lymph nodes of goats by use of selective Dubos medium. *J Clin Microbiol* 1985; 22: 312–3.

75. Schena M, Shalon D, Davis RW. Quantitative monitoring of gene expression patterns with a complementary DNA microarray. *Science* 1995; 270(5235): 467-70.

76. Schwartz D, Shafran I, Romero C, et al. Use of short-term culture for identification of *Mycobacterium avium* subsp. *paratuberculosis* in tissue from Crohn's disease patients. *Clin Microbiol Infect* 2000; 6: 303–7.

77. Shafran I, Piromalli C, Decker JW, et al. Seroreactivities against *Saccharomyces cerevisiae* and *Mycobacterium avium* subsp. *paratuberculosis* p35 and p36 antigens in Crohn's disease patients. *Dig Dis Sci.* 2002;47(9):2079-81.

78. Sweeney RW, Whitlock RH, Rosenberger AE. *Mycobacterium paratuberculosis* cultured from milk and supramammary lymph nodes of infected asymptomatic cows. *J Clin Microbiol* 1992; 30: 166–71.

79. Tissot C, Mechti N. Molecular cloning of a new interferon-induced factor that represses human immunodeficiency virus type 1 long terminal repeat expression. *J Biol Chem.* 1995; 270(25): 14891-8.

80. Vidal Pessolani MC, Marques MA, Reddy VM, et al. Systemic dissemination in tuberculosis and leprosy: do mycobacterial adhesins play a role? *Microbes Infect.* 2003; 5(7): 677-84.

81. Whitney A, Diehn M, Popper S, et al. Individuality and variation in gene expression patterns in human blood. *Proc Natl Acad Sci.* 2003; 100:1896-1901.

82. Wu SWP, Pao CC, Chan J. Lack of mycobacterial DNA in Crohn's disease tissue. *Lancet* 1991; 337: 174-175.

83. Wu LC. ZAS: C2H2 zinc finger proteins involved in growth and development. *Gene Expression* 2002; 10: 137-152.

84. Wu MY, Wang PY, Han SH, et al. The cytoplasmic domain of the lymphotoxin-beta receptor mediates cell death in HeLa cells. *J Biol Chem* 1999; 274 (17): 11868-73.

85. Yamamora M, Uyemura K, Deans RJ, et al. Defining Protective Responses to Pathogens: Cytokine Profiles in Leprosy Lesions. *Science.* 1991; 254: 277-279.

86. Yoshimura HH, Graham DY, Estes MK, et al. Investigation of association of Mycobacteria with inflammatory bowel disease by nucleic acid hybridization. *J. Clin. Microbiol.* 1987; 25:45-51.